

DOE/ER/40561-257-INT96-00-125  
 UW/PT 96-06  
 CMU-HEP96-06  
 DOE-ER-40862-117  
 CALT-68-2047

# Nucleon-Nucleon Scattering from Effective Field Theory

David B. Kaplan

*Institute for Nuclear Theory, University of Washington*  
*Box 351550, Seattle WA 98195-1550*  
 dbkaplan@phys.washington.edu

Martin J. Savage <sup>†</sup>

*Department of Physics, Carnegie Mellon University, Pittsburgh PA 15213*  
 savage@thepub.phys.cmu.edu

Mark B. Wise

*California Institute of Technology, Pasadena, CA 91125*  
 wise@theory.caltech.edu

We perform a nonperturbative calculation of the  $^1S_0$   $NN$  scattering amplitude, using an effective field theory (EFT) expansion. The expansion we advocate is a modification of what has been used previously; it is not a chiral expansion in powers of  $m_\pi$ . We use dimensional regularization throughout, and the  $\overline{MS}$  renormalization scheme; our final result depends only on physical observables. We show that the EFT expansion of the quantity  $|\mathbf{p}| \cot \delta(\mathbf{p})$  converges at momenta much greater than the scale  $\Lambda$  that characterizes the derivative expansion of the EFT Lagrangian. Our conclusions are optimistic about the applicability of an EFT approach to the quantitative study of nuclear matter.

5/96

---

<sup>†</sup> DOE Outstanding Junior Investigator. Address after Sept. 1, 1996: Dept. of Physics, University of Washington, Box 351550, Seattle WA 98195-1550.

## 1. Introduction

Effective field theories are routinely used in particle physics and have proved an invaluable tool for computing physical quantities in theories with disparate energy scales [1] (for recent reviews see [2]). Several years ago, Weinberg proposed that the machinery of effective field theory (EFT) could be applied fruitfully to nucleon-nucleon scattering and nuclear physics [3]. Nucleon interactions might be profitably treated by EFT since they involve several different physical scales, such as the nucleon mass  $M$ , the pion and vector meson masses ( $m_\pi$ ,  $m_\rho$ ,  $m_\omega$ , etc.). Furthermore, chiral symmetry in nucleon-pion interactions is necessarily expressed in the language of EFT, and the chiral expansion around  $m_\pi = 0$  gives one a natural expansion parameter. Since Weinberg's original papers, much work has been done in the subject, with fair success in reproducing low energy features of nucleon-nucleon scattering from a chiral Lagrangian description of nucleon interactions [4] [5].

The goal of an EFT description of nuclear physics is not to improve upon semi-phenomenological models of the nucleon-nucleon interaction, such as the Paris [6], Bonn [7] or Nijmegen [8] potentials. Instead it has been used to relate 3-body forces to 2-body forces [3][5] and to explain the observed hierarchy of isospin violation [9]. One can also investigate the role of strangeness in hypernuclei or dense matter, along the lines of [10]. More generally, it allows one to better understand the physical origin of various features of the nucleon interaction (for recent progress in this direction see [11-14] and references therein). One may also hope that the technique will allow semi-analytical approaches to solving 2- and many-body problems now only approached numerically.

A fundamental difficulty in an EFT description of nuclear forces is that they are necessarily nonperturbative, so that an infinite series of Feynman diagrams must be summed. Which diagrams must be summed is well known, and the summing them is equivalent to solving a Schrödinger equation. However, an EFT yields graphs which require renormalization, giving rise to a Schrödinger potential which is too singular to solve conventionally. In Weinberg's work [3], only a contact interaction was summed, and the system was renormalized; in [4][5][9], more complicated interactions are considered and a momentum cut-off is implemented, with bare couplings chosen to best fit phase shift data. In this paper we

focus on the  $^1S_0$  ( $np$ ) partial wave, and show how to compute the phase shift beyond lowest order in the EFT expansion, using dimensional regularization and the minimal subtraction ( $\overline{MS}$ ) renormalization scheme.

Another problem with discussing systems with barely bound (or nearly bound) states in the language of EFT is that a new length scale emerges that is not directly associated with any physical threshold — the scattering length  $a$ . This makes the power counting in an EFT with large scattering length much less obvious than in one without.  $^1S_0$  nucleon-nucleon scattering is particularly problematic from an effective field theory point of view, since the scattering length is very large:  $a \sim -24 \text{ fm} \sim (8.5 \text{ MeV})^{-1}$ , a mass scale far lower than any hadron mass. In this paper we propose a specific ordering of the EFT expansion to avoid this problem. In the process, we are led to a modification of the power counting scheme proposed by Weinberg.

We begin by briefly reviewing Weinberg’s power counting scheme and the connection between Feynman diagrams and the Schrödinger equation. We then show how to sum the relevant graphs even when they are divergent, and we construct the low energy EFT for nucleons alone in the  $\overline{MS}$  scheme. Finally we construct the EFT including one pion exchange in the  $\overline{MS}$  scheme; in both cases we show at what scale the EFT fails. We conclude with thoughts about improving the approach, and its applicability to finite density calculations.

## 2. Effective field theory, power counting and the Schrödinger equation

### 2.1. Weinberg’s power counting scheme

The philosophy of EFT is that for scattering processes involving external momenta  $\lesssim Q$ , one need only consider a Lagrangian which explicitly includes light degrees of freedom for which  $m \lesssim Q$ . The effects of heavy virtual particles appear as an infinite number of nonrenormalizable operators suppressed by powers of the mass scale  $\Lambda$  relevant to the degrees of freedom excluded from the theory. EFT’s can be predictive since amplitudes may be expanded in powers of  $Q/\Lambda$ , so that the effect of a nonrenormalizable operator on low energy physics is less important the higher the dimension of that operator.

The scale  $\Lambda$  can be determined by fitting low energy data to the predictions of the EFT to sufficient accuracy; the lower the scale  $\Lambda$ , the smaller the momentum range over which the EFT is predictive. An EFT will have to be modified as one approaches  $Q \simeq \Lambda$ , and the degrees of freedom with mass  $\Lambda$  must then be explicitly included in the EFT. One then has a new EFT characterized by a scale  $\Lambda'$ , which characterizes the next level of particles excluded from the theory. An EFT is only useful to the extent that there is a well defined hierarchy of mass scales; if there is such a hierarchy one can typically predict a large amount of data in terms of a few parameters.

A necessary ingredient for an EFT is a power counting scheme that tells one what graphs to compute to any order in the momentum expansion. We reproduce here Weinberg's analysis for  $NN$  scattering, couched however in the language of covariant rather than time ordered perturbation theory. The main complication arises from the fact that a nucleon propagator  $S(q) = i/(q_0 - \mathbf{q}^2/2M)$  scales like  $1/Q$  if  $q_0$  scales like  $m_\pi$  or an external 3-momentum, while  $S(q) \sim M/Q^2$  if  $q_0$  scales like an external kinetic energy. Similarly, in loops  $\int dq_0$  can scale like  $Q$  or  $Q^2/M$ , depending on which type of pole is picked up. To distinguish between these two scaling properties we begin by defining generalized “ $n$ -nucleon potentials”  $V^{(n)}$  comprised of those parts of connected Feynman diagrams with  $2n$  external nucleon lines that have no powers of  $M$  in their scaling<sup>1</sup>. Such a diagram always has exactly  $n$  nucleon lines running through it, since there is no nucleon-antinucleon pair creation in the effective theory.  $V^{(n)}$  includes (i) diagrams which are  $n$ -nucleon irreducible; (ii) parts of diagrams which are 1-nucleon irreducible<sup>2</sup>. To compute the latter contribution to  $V^{(n)}$  one identifies all combinations of two or more internal nucleon lines that can be simultaneously on-shell, and excludes their pole contributions when performing the  $\int dq_0$  loop integrations. An example of the 2-pion exchange contributions to  $V^{(2)}$  is shown in Fig. 1.

A special comment must be made about the 1-nucleon potentials,  $V^{(1)}$ . These diagrams consist solely of the 1-nucleon irreducible graphs. They include both wave function

---

<sup>1</sup> With the exception of inverse powers of  $M$  from relativistic corrections.

<sup>2</sup> An  $n$ -nucleon irreducible diagram is one which does not fall apart when  $n$  nucleon lines are cut.

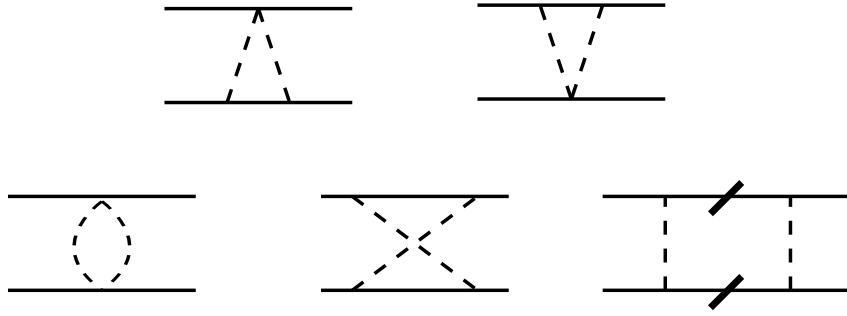


Fig. 1. One loop, 2-pion exchange Feynman graphs which contribute to the 2-nucleon potential  $V^{(2)}$ . The first four are 2-nucleon irreducible; the last diagram is 2-nucleon reducible, and the poles from the slashed propagators are not included in the  $\int dq_0$  loop integration. The 1-loop graphs corresponding to  $\pi NN$  vertex renormalization and pion wave function renormalization are not pictured here, but enter at the same order (as does nucleon wave function renormalization).

renormalization (which begins at order  $Q^2$ ) as well as relativistic corrections to the nucleon propagator, which start at order  $Q^4/M^3$ . The structure of the latter terms is fixed by relativistic invariance to reproduce the Taylor expansion of  $\sqrt{\mathbf{p}^2 + M^2}$ .

A general  $n$ -nucleon Feynman diagram in the EFT can be constructed by sewing together the nucleon legs of  $V^{(r)}$  potentials with  $r \leq n$ ; one treats the  $V^{(r)}$ 's like vertices and the  $\int dq_0$  loop integrations pick up the poles of all the connecting nucleon lines<sup>3</sup>.

The reason for this construction is that within the  $V^{(r)}$  potentials, all nucleon propagators are off-shell and scale like  $1/q_0 \sim 1/Q$ . In contrast, when one picks up the pole contribution from one of the nucleon lines connecting the  $V^{(r)}$  “vertices”, other nucleon lines will be almost on-shell, and scale like  $1/(Q^2/M)$ .

Following Weinberg's arguments [3], a contribution to the  $r$ -nucleon potential  $V^{(r)}$  with  $\ell$  loops,  $I_n$  nucleon propagators,  $I_\pi$  pion propagators, and  $V_i$  vertices involving  $n_i$

---

<sup>3</sup> As pointed out by Weinberg, this set of diagrams is more naturally described in the language of time-ordered perturbation theory, but as there will be a mix of relativistic pion propagators and nonrelativistic nucleon propagators, no formalism is ideal, and we will keep to the language of covariant perturbation theory.

nucleon lines and  $d_i$  derivatives, scales like  $Q^\mu$ , where

$$\mu = 4l - I_n - 2I_\pi + \sum V_i d_i , \quad (2.1a)$$

$$\ell = I_n + I_\pi - \sum V_i + 1 , \quad (2.1b)$$

$$I_n + r = \frac{1}{2} \sum V_i n_i . \quad (2.1c)$$

In this power counting we take  $m_\pi \sim Q$  and treat factors of the  $u$  and  $d$  quark masses at the vertices as order  $Q^2$ . Combining these relations leads to the scaling law for the  $r$ -nucleon potential  $V^{(r)}$  ( $r \geq 2$ ):

$$\mu = 2 + 2\ell - r + \sum_i V_i (d_i + \frac{1}{2}n_i - 2) . \quad (2.2)$$

Since chiral symmetry implies that the pion is derivatively coupled, it follows that  $(d_i + \frac{1}{2}n_i - 2) \geq 0$ . That implies that for a 2-nucleon potential,  $\mu \geq 0$ , and that  $\mu = 0$  corresponds to tree diagrams.

It is straight forward to find the scaling property for a general Feynman amplitude, by repeating the analysis that leads eq. (2.2), treating the  $V^{(r)}$  potentials as  $r$ -nucleon vertices with  $\mu$  derivatives,  $\mu$  given by eq. (2.2). However, while eq. (2.2) was derived assuming that  $\int dq_0 \sim Q$  and nucleon propagators scaled like  $\sim 1/Q$ , we now take them to scale like  $Q^2/M$  and  $1/(Q^2/M)$  respectively. A general Feynman diagram is constructed by stringing together  $r$ -nucleon potentials  $V^{(r)}$ .

For two nucleon scattering the situation is particularly simple, since the diagrams are all ladder diagrams, with  $n$  insertions of  $V^{(2)}$ 's acting as ladder rungs. Each loop of the ladder introduces a loop integration ( $dq_0 d^3\mathbf{q} \sim Q^5/M$ ) and two nucleon propagators ( $\sim M^2/Q^4$ ) to give a net factor of  $(QM)$  per loop. If we expand  $V^{(2)} = \sum_{\mu=0}^{\infty} V_\mu^{(2)}$ , where  $V_\mu^{(2)} \sim Q^\mu$ , then a 2-nucleon diagram whose  $i^{th}$  rung is the generalized potential  $V_{\mu_i}^{(2)}$  scales as

$$Q^\nu (QM)^L , \quad \nu = \sum_{i=1}^{L-1} \mu_i , \quad (2 - \text{body scattering}) \quad (2.3)$$

where  $L$  is the number of loops (external to the  $V^{(2)}$ 's). With insertions of  $V^{(1)}$  along the nucleon propagators, which serve as relativistic corrections, there will be additional powers

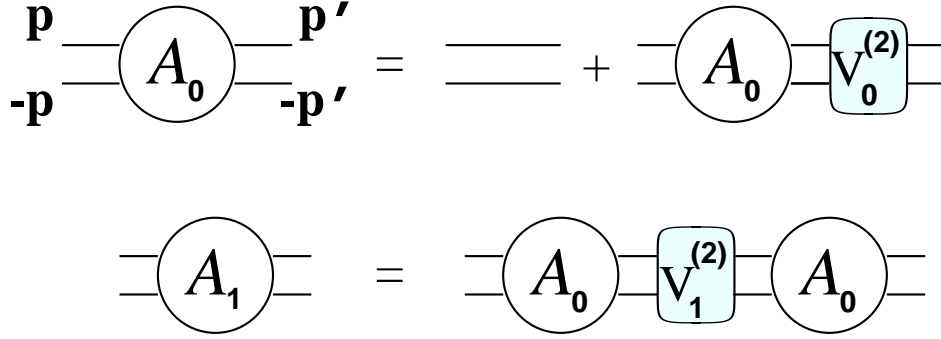


Fig. 2. The first two terms in the EFT expansion for the Feynman amplitude (T-matrix) for nucleon-nucleon scattering in the center of mass frame. The leading amplitude  $\mathcal{A}_0$  scales like  $Q^0$  and consists of the sum of ladder diagrams with the leading ( $\mu = 0$ ) 2-nucleon potential  $V_0^{(2)}$  at every rung; the subleading amplitude  $\mathcal{A}_1$  scales like  $Q$ ; it consists one insertion of  $V_1^{(1)}$  (1-loop nucleon wavefunction renormalization) or one insertion of the subleading ( $\mu = 1$ ) 2-nucleon potential  $V_1^{(2)}$ , dressed by all powers of the leading interaction  $V_0^{(2)}$ .

of  $(Q^2/M^2)$ ; likewise, an expansion of retardation effects in  $V^{(2)}$  can be treated like the nonrelativistic expansion.

Since  $\mu_i \geq 0$ , the leading behaviour of the 2-nucleon amplitude is  $(QM)^L$ . If one treats  $M \simeq Q^0$ , it follows that perturbation theory is adequate for describing the 2-nucleon system at low  $Q$ . In order to explain the nonperturbative effects one sees (*e.g.*, the deuteron, or the large scattering length in the  $^1S_0$  channel) one must conclude that  $M \simeq 1/Q$  in a consistent power counting scheme. Thus the effective field theory calculation must be an expansion in  $\nu$ , given by eqs. (2.2), (2.3). To leading order ( $\nu = 0$ ) one must sum up all ladder diagrams with insertions of  $V_0^{(2)}$  potentials with  $\mu = 0$ . At subleading order one includes one insertion of  $V_1^{(2)}$  and all powers of  $V_0^{(2)}$ , etc.

The program advocated by Weinberg is to solve the Schrödinger equation with the kernel  $V^{(2)}$  expanded to a given order in  $\mu$ . An alternative one might consider is to expand the Feynman amplitude  $\mathcal{A}$  in powers of  $\nu$ ; this is an equivalent procedure at  $\nu = 0$ , but is unsatisfactory for higher  $\nu$  as the expansion violates unitarity. We will argue in subsequent sections that for systems with a large scattering length (*e.g.*  $NN$  scattering) the best procedure is to expand  $|\mathbf{p}| \cot \delta(\mathbf{p}) = (4\pi/M)\text{Re}[1/\mathcal{A}]$  in powers of  $\nu$ , where  $\mathbf{p}$

is the momentum in the center of mass frame, and  $\delta$  is the phase shift. As discussed below, this expansion preserves unitarity and is expected to converge much faster than the expansion of the kernel  $V^{(2)}$ , particularly in systems with a large scattering length.

A further modification we propose below is in the basic power counting scheme. In particular, we will argue that there are explicit powers of  $M$  in the coefficients of operators of the EFT, which decreases their order in the EFT expansion. We return to this point below, once we have presented the calculational techniques that lead to this result.

## 2.2. Feynman diagrams and the Schrödinger equation

Feynman diagrams are the usual tool for computing perturbative amplitudes requiring renormalization, while the Schrödinger equation is used to solve nonperturbative problems in potential scattering. As we will need to do both simultaneously, we briefly review here the connection between Feynman diagrams and the Schrödinger equation.

Consider the integrals arising from the ladder loops in the diagrams of fig. 2:

$$I = \int \frac{d^4q}{(2\pi)^4} V^{(2)}(p, q) \frac{i}{(E/2 + q_0 - \mathbf{q}^2/2M + i\epsilon)} \frac{i}{(E/2 - q_0 - \mathbf{q}^2/2M + i\epsilon)} V^{(2)}(q, p') . \quad (2.4)$$

In the above expression,  $M$  is the nucleon mass,  $E$  is the center of mass kinetic energy. (As we will focus entirely on the 2-nucleon problem for the rest of the paper, we will henceforth refer to the 2-nucleon potential  $V^{(2)}$  simply as  $V$ ). Following the rules of the previous section, the  $\int dq_0$  integral only picks up the pole contribution from the nucleon propagators at  $q_0 = \pm(E/2 - \mathbf{q}^2/2M)$ . Since  $q_0 \sim Q^2/M$  one can consistently take  $q_0 \sim 0$  in  $V$  (*i.e.*, ignore retardation) to the order we will be working. In this approximation

$$I \sim i \int \frac{d^3\mathbf{q}}{(2\pi)^3} V(\mathbf{p}, \mathbf{q}) \frac{1}{(E - \mathbf{q}^2/M + i\epsilon)} V(\mathbf{q}, \mathbf{p}') . \quad (2.5)$$

The connection between the above expression and the Schrödinger equation is clarified by defining the free retarded Schrödinger Green's function operator for the 2-nucleon system

$$\hat{G}_E^0 = \frac{1}{(E - \hat{H}_0 + i\epsilon)} , \quad \hat{H}_0 = \frac{\mathbf{p}^2}{M} , \quad (2.6)$$

Matrix elements of  $\hat{G}_E^0$  and the potential operator,  $\hat{V}$ , between momentum eigenstates are given by

$$\langle \mathbf{p} | \hat{G}_E^0 | \mathbf{p}' \rangle = \frac{(2\pi)^3 \delta^3(\mathbf{p} - \mathbf{p}')}{(E - \mathbf{p}^2/M + i\epsilon)} , \quad \langle \mathbf{p} | \hat{V} | \mathbf{p}' \rangle = V(\mathbf{p}, \mathbf{p}') . \quad (2.7)$$



The sum of ladder diagrams can then be expressed as

$$\begin{aligned}
i\mathcal{A} &= -i \langle \mathbf{p} | \left( \hat{V} + \hat{V} \hat{G}_E^0 \hat{V} + \hat{V} (\hat{G}_E^0 \hat{V})^2 + \dots \right) | \mathbf{p}' \rangle \\
&= -i \langle \mathbf{p} | \hat{V} (1 + \hat{G}_E \hat{V}) | \mathbf{p}' \rangle \\
&= -i \langle \mathbf{p} | (\hat{G}_E^0)^{-1} \hat{G}_E (\hat{G}_E^0)^{-1} | \mathbf{p}' \rangle ,
\end{aligned} \tag{2.8}$$

where  $\hat{G}_E$  is the full Green's function with potential  $\hat{V}$ :

$$\hat{G}_E = \frac{1}{(E - \hat{H} + i\epsilon)} , \quad \hat{H} = \hat{H}_0 + \hat{V} . \tag{2.9}$$

We can define the state

$$|\chi_{\mathbf{p}}\rangle \equiv (1 + \hat{G}_E \hat{V}) | \mathbf{p} \rangle = \hat{G}_E (\hat{G}_E^0)^{-1} | \mathbf{p} \rangle \tag{2.10}$$

with  $\mathbf{p}^2/M = E$ , which is seen to be the exact scattering solution of interest: it satisfies the full Schrödinger equation since

$$(\hat{H} - E) |\chi_{\mathbf{p}}\rangle = -\hat{G}_E^{-1} |\chi_{\mathbf{p}}\rangle = (\hat{H}_0 - E) | \mathbf{p} \rangle = 0 , \tag{2.11}$$

and takes the appropriate asymptotic form for large  $r$

$$\chi_{\mathbf{p}}(\mathbf{r}) \rightarrow e^{i\mathbf{p}\cdot\mathbf{r}} + \frac{f(\theta, \phi)}{r} e^{i\mathbf{p}r} , \tag{2.12}$$

since  $\langle r | \hat{G}_E \hat{V} | r' \rangle \propto 1/r$  for large  $r$ . The Feynman amplitude (2.8) can be expressed in terms of  $\chi$  as

$$i\mathcal{A} = -i \int d^3r e^{-i\mathbf{p}\cdot\mathbf{r}} V(\mathbf{r}) \chi_{\mathbf{p}'}(\mathbf{r}) , \tag{2.13}$$

which is  $(-i)$  times the conventional expression for the  $T$ -matrix (see, for example, [15]). For  $s$ -wave scattering at center of mass momentum  $\mathbf{p}$ ,  $\mathcal{A}$  can be conveniently related to the phase shift  $\delta(\mathbf{p})$  by the relation

$$\begin{aligned}
|\mathbf{p}| \cot \delta(\mathbf{p}) &= i|\mathbf{p}| + \frac{4\pi}{M} \frac{1}{\mathcal{A}} \\
&= -\frac{1}{a} + \frac{1}{2} r_0 \mathbf{p}^2 + \dots ,
\end{aligned} \tag{2.14}$$

where  $a$  is the scattering length and  $r_0$  is the effective range. For  $^1S_0$  ( $np$ ) scattering, these parameters are measured to be (see [16])

$$a = -23.714 \pm 0.013 \text{ fm} , \quad r_0 = 2.73 \pm 0.03 \text{ fm} . \tag{2.15}$$

The above discussion is complete when the potential  $V$  is less singular than  $1/r^2$  at the origin, in which case the terms in the series of eq. (2.8) are well defined. However, in effective field theories, the potential will in general have more singular behavior, such as  $1/r^2$ ,  $1/r^3$ ,  $\delta^3(\mathbf{r})$ , and worse. Such potentials do not allow a conventional solution to the Schrödinger equation, or equivalently, lead to divergent diagrams in the field theory. In the field theory it is well known how to deal with divergences — one merely regulates the integrals and then renormalizes the couplings of the theory, absorbing terms that diverge as the cutoff is removed into the definitions of the renormalized couplings. When this is done, there is no cutoff dependence in the theory. In this paper, we show how to sum up the leading diagrams using dimensional regularization and the  $\overline{MS}$  subtraction scheme for the case of  $^1S_0$  nucleon-nucleon scattering. This is equivalent to solving the dimensionally regulated Schrödinger equation. The advantages of our procedure are that dimensional regularization with the  $\overline{MS}$  scheme preserves chiral symmetry and simplifies computations. Since the renormalization scale  $\mu$  introduced by  $\overline{MS}$  (or any mass independent scheme, such as  $MS$ ) only enters in logarithms, EFT power counting arguments are particularly transparent, unlike when a momentum cutoff procedure is used.

### 3. The effective theory with nucleons alone

Although the power counting of the previous section assumed  $Q \sim m_\pi$  and explicitly included pion propagation, the analysis also applies to a lower  $Q$  regime where the pion plays no role. We analyze this case first as it is analytically more accessible and quite instructive.

At very low energy  $NN$  scattering we may consider an effective field theory consisting solely of nucleon fields; all other degrees of freedom, such as  $\pi$ 's,  $\Delta$ 's,  $\rho$  and  $\omega$  mesons have been integrated out, and their effects are subsumed in the coupling constants of the effective theory. Note that this effective theory has nothing to do with chiral symmetry; in fact, it treats the pion as very heavy compared to momenta of interest, which is the opposite of the chiral limit.

The EFT consists of all local nucleon interactions allowed by rotational invariance, isospin symmetry (which we assume to be exact in this paper) and parity. For 2-nucleon

scattering, the only interactions that are of relevance are the operators with four nucleon fields, as well as relativistic corrections to the nucleon propagator; we will be able to ignore the latter to the order we are working. In such a theory, the only diagrams that contribute to the 2-body potential  $V$  are tree diagrams. It follows from eq. (2.2) that each 4-nucleon operator has a scaling dimension  $\mu_i = d_i$ , where  $d_i$  is the number of derivatives in the acting at the vertex. Eq. (2.3) then tells us that the leading contribution to the amplitude has  $\nu = 0$ , and that  $\mathcal{A}_0$  is given by the bubble sum of 4-nucleon operators with no derivatives. At  $\nu = 2$ ,  $\mathcal{A}_2$  is given by one insertion of a 2-derivative, 4-nucleon operator, dressed by the no-derivative operator, as in fig. 2, etc.

The effective Lagrangian for this theory is given by

$$\begin{aligned} \mathcal{L} = & N^\dagger i \partial_t N - N^\dagger \frac{\nabla^2}{2M} N - \frac{1}{2} C_S (N^\dagger N)^2 - \frac{1}{2} C_T (N^\dagger \vec{\sigma} N)^2 \\ & - \frac{1}{4} C_2 (N^\dagger \nabla^2 N) (N^\dagger N) + h.c. + \dots \end{aligned} \quad (3.1)$$

where  $\vec{\sigma}$  are the Pauli matrices acting on spin indices, and the ellipses refer to additional 4-nucleon operators involving two or more derivatives, as well as relativistic corrections to the propagator. The coefficients  $C_S$  and  $C_T$  of dimension  $(\text{mass})^{-2}$  are the couplings introduced by Weinberg [3];  $C_2$  is a coupling of dimension  $(\text{mass})^{-4}$ . The values of  $C_S$ ,  $C_T$ ,  $C_2$  are renormalization scheme dependent.

Nucleon scattering in the  $^1S_0$  channel only depends on  $C_S$  and  $C_T$  in the linear combination  $C = (C_S - 3C_T)$ , and so the leading contribution to the potential is

$$V_0(\mathbf{p}, \mathbf{p}') = C. \quad (3.2)$$

Similarly, one can show that while there are a number of operators with four nucleon fields and two derivatives, only the linear combination proportional to  $C_2$  in eq. (3.1) contributes to  $V_2$  in the  $^1S_0$  channel. It will be convenient for later discussion of the momentum expansion to define

$$C_2 \equiv \frac{C}{\Lambda^2}, \quad (3.3)$$

where  $\Lambda$  is a parameter with dimension of mass. With this definition the next to leading order contribution to the 2-nucleon potential is

$$V_2(\mathbf{p}, \mathbf{p}') = C \left( \frac{\mathbf{p}^2 + \mathbf{p}'^2}{2\Lambda^2} \right). \quad (3.4)$$

### 3.1. The $\nu = 0$ calculation

The ladder graphs in fig. 2 for the leading part of the amplitude  $\mathcal{A}_0$  can be summed trivially with the kernel  $V_0$  in eq. (3.2), since the expression (2.8) is a geometric series. Using dimensional regularization one finds

$$i\mathcal{A}_0 = \frac{-iC}{1 - C\tilde{G}_E^0(\mathbf{0}, \mathbf{0})} = \frac{-iC}{1 + iCM|\mathbf{p}|/4\pi}. \quad (3.5)$$

The quantity

$$\tilde{G}_E^0(\mathbf{0}, \mathbf{0}) = \int \frac{d^n \mathbf{q}}{(2\pi)^n} \int \frac{d^n \mathbf{q}'}{(2\pi)^n} \langle \mathbf{q} | \hat{G}_E^{(0)} | \mathbf{q}' \rangle, \quad (3.6)$$

is simply the coordinate space representation of the free Green's function  $\tilde{G}_E^0(\mathbf{r}, \mathbf{r}') = \langle \mathbf{r} | 1/(E - \hat{H}_0 + i\epsilon) | \mathbf{r}' \rangle$  evaluated at  $\mathbf{r} = \mathbf{r}' = 0$ , with reduced mass  $M/2$ . This corresponds to a divergent one loop graph, which in dimensional regularization is given by:

$$\begin{aligned} \tilde{G}_E^0(\mathbf{0}, \mathbf{0}) &= \int \frac{d^n \mathbf{q}}{(2\pi)^n} \frac{1}{(E - \mathbf{q}^2/M + i\epsilon)} \\ &= - (4\pi)^{-n/2} M(-ME - i\epsilon)^{(n-2)/2} \Gamma(1 - n/2) \\ &\xrightarrow{n \rightarrow 3} \frac{M\sqrt{-ME - i\epsilon}}{4\pi} = \frac{-iM|\mathbf{p}|}{4\pi}. \end{aligned} \quad (3.7)$$

Even though minimal subtraction introduces a renormalization scale  $\mu$ , one finds that in dimensional regularization  $\tilde{G}_E^0(\mathbf{0}, \mathbf{0})$  is finite as  $n \rightarrow 3$  and so  $C$  is independent of  $\mu$ , satisfying the trivial renormalization group (RG) equation

$$\mu \frac{\partial}{\partial \mu} \left( \frac{1}{C} \right) = 0. \quad (3.8)$$

The value of  $C$  is determined by experiment via eq. (2.14) which fixes the threshold amplitude to be  $\mathcal{A} = -4\pi a/M$ , where  $a$  is the scattering length. It follows from eqs. (3.5) and (3.7), using  $M = 940\text{MeV}$ , that

$$C = \frac{4\pi a}{M} = - \left( \frac{1}{25 \text{ MeV}} \right)^2. \quad (3.9)$$

The expression for the scattering amplitude (3.5) may be rewritten as

$$i\mathcal{A}_0 = i \frac{4\pi/M}{-1/a - i|\mathbf{p}|}, \quad (3.10)$$

which is recognized as the effective range theory expression for the amplitude given a scattering length  $a$  and effective range  $r_0 = 0$ :

$$|\mathbf{p}| \cot \delta(\mathbf{p}) = -\frac{1}{a} . \quad (3.11)$$

This is reasonable, since the interaction (3.1) is local. In fact, it is shown in the appendix how (3.9) may be derived by solving the Schrödinger equation with a potential  $V(\mathbf{r}) = C\delta^{(3)}(\mathbf{r})$ .

### 3.2. The $\mu = 2$ calculation

When using an effective Lagrangian, it is important to know at what momentum it fails. The momentum expansion in the effective Lagrangian (3.1) breaks down at the scale  $Q \sim \Lambda$ , where  $\Lambda$  is the scale set by  $V_2$  (3.4). To determine  $\Lambda$ , we must perform a second order calculation, at  $\nu = 2$ . How to do so is ambiguous: if one expands the Feynman amplitude to order  $\nu = 2$  as in fig. 2, one destroys unitarity. In this section we will follow Weinberg's prescription, namely to expand  $V$  to second order (*i.e.*,  $\mu = 2$ ), and then sum its effects on the amplitude to all order. Doing so includes the exact expressions for the order  $\nu = 0$  and  $\nu = 2$  parts of the full amplitude, and keeps parts of the higher order terms (from multiple insertions of  $V_2$ ). In the following section we will consider an alternative calculation.

To next to leading order, the 2-nucleon potential  $V$  is given by

$$V(\mathbf{p}, \mathbf{p}') = V_0 + V_2 = C \left( 1 + \frac{\mathbf{p}^2 + \mathbf{p}'^2}{2\Lambda^2} \right) . \quad (3.12)$$

It is possible to sum all of the ladder diagrams with the vertex (3.12) in the  $\overline{MS}$  scheme; as shown in appendix B, one merely replaces  $C$  in eq. (3.5) by  $C(1 + \mathbf{p}^2/\Lambda^2)$ :

$$i\mathcal{A}_{V_2} = \frac{-i}{1/[C(1 + \mathbf{p}^2/\Lambda^2)] + iM|\mathbf{p}|/4\pi} , \quad (3.13)$$

where the subscript  $V_2$  denotes that we have followed Weinberg's prescription and expanded  $V$  (rather than  $\mathcal{A}$ ) to subleading order  $\mu = 2$ . Since  $E = \mathbf{p}^2/M$ , the above expression for the amplitude can be expressed as a prediction for  $|\mathbf{p}| \cot \delta(\mathbf{p})$  by means of eq. (2.14):

$$|\mathbf{p}| \cot \delta(\mathbf{p}) = - \left( \frac{4\pi}{M} \right) \frac{1}{C(1 + \mathbf{p}^2/\Lambda^2)} . \quad (3.14)$$

We can fit our two free parameters  $C$  and  $\Lambda^2$  to low energy scattering data by expanding  $|\mathbf{p}| \cot \delta(\mathbf{p})$  to order  $\mathbf{p}^2$  and fitting to the measured scattering length and effective range (2.15). The result is

$$C = \frac{4\pi a}{M} = - \left( \frac{1}{25 \text{ MeV}} \right)^2, \quad \frac{1}{\Lambda^2} = \frac{1}{2} r_0 a = - \left( \frac{1}{35 \text{ MeV}} \right)^2. \quad (3.15)$$

Since  $\mathbf{p} \simeq \Lambda$  is the scale at which  $V_0 \simeq V_2$ , we expect the effective theory with nucleons alone to work well at center of mass momenta  $|\mathbf{p}| \ll 35 \text{ MeV}$ , but to fail completely for  $|\mathbf{p}| \gtrsim 35 \text{ MeV}$ , corresponding to the lab kinetic energy  $T_{\text{lab}} = 2.6 \text{ MeV}$ .

### 3.3. An alternative: expanding $|\mathbf{p}| \cot \delta(\mathbf{p})$ to order $\nu = 2$

The result (3.15) is very discouraging from the EFT point of view. The original premise in §2 was that amplitudes could be expanded in powers of  $(Q/\Lambda)^\nu$ , where  $\Lambda$  was a mass scale typical of the particles not included explicitly in the theory. When pions are included, we would hope that  $\Lambda \sim m_\rho$ ; in the lower energy EFT we are considering here, with the pion integrated out, one would expect  $\Lambda \sim m_\pi$ . Instead, eq. (3.15) has  $\Lambda \sim 1/\sqrt{ar_0}$ ;  $r_0$  can be considered a relatively short distance scale, but  $a \sim -1/(8 \text{ MeV})$  for the  $^1S_0$  channel, which can hardly be called a typical QCD scale. In general,  $a$  blows up as a bound state (or nearly bound state) approaches threshold. Thus a small change in short distance physics can make the EFT fail at arbitrarily low momenta.

The problem can be made more precise by examining the quantity  $|\mathbf{p}| \cot \delta(\mathbf{p})$ . Eqs. (3.14) and (3.15) imply that

$$|\mathbf{p}| \cot \delta(\mathbf{p}) = \frac{1}{-a + \frac{1}{2} a^2 r_0 \mathbf{p}^2} = -\frac{1}{a} \sum_{n=0}^{\infty} \left( -\frac{1}{2} a r_0 \mathbf{p}^2 \right)^n, \quad (3.16)$$

which has a radius of convergence at  $\mathbf{p}^2 \sim 1/(ar_0)$ . However, it is known from general arguments that for a potential that falls off exponentially as  $e^{-mr}$  for large  $r$ , the true radius of convergence for  $|\mathbf{p}| \cot \delta(\mathbf{p})$  is given by  $\mathbf{p}^2 \sim m^2$  [15]. The quantity  $|\mathbf{p}| \cot \delta(\mathbf{p})$  should have an expansion of the form

$$|\mathbf{p}| \cot \delta(\mathbf{p}) \sim -\frac{1}{a} + \frac{1}{2} r_0 \mathbf{p}^2 \sum_{n=0}^{\infty} (r_n^2 \mathbf{p}^2)^n, \quad (3.17)$$

where the scales  $r_n$  are typical of the range of the potential,  $r_0 \sim r_n \sim 1/m$ . None of the  $r_n$ 's are expected to diverge as  $|a| \rightarrow \infty$ .

How are we to reconcile eq. (3.17) with our discovery in eq. (3.16) that the scale of momentum variation in the EFT is set by the length scale  $\sqrt{ar_0}$ ? The only possible answer is that the higher derivative operators in the EFT, although controlled by a scale that diverges as  $|a| \rightarrow \infty$ , are actually highly correlated, and the effects that diverge with  $a$  cancel. To see how this works in the present theory, consider a different expansion than the one performed above: instead of expanding  $V$  to order  $\mu = 2$  and solving for the amplitude, we will expand  $|\mathbf{p}| \cot \delta(\mathbf{p})$  to order  $\nu = 2$ . In terms of a  $\nu$  expansion of the Feynman amplitude (as in fig. 2)

$$\mathcal{A} = \mathcal{A}_0 + \mathcal{A}_1 + \mathcal{A}_2 + \dots, \quad (3.18)$$

the expansion of  $|\mathbf{p}| \cot \delta(\mathbf{p})$  is given by

$$\begin{aligned} |\mathbf{p}| \cot \delta(\mathbf{p}) &= i|\mathbf{p}| + \frac{4\pi}{M} \frac{1}{\mathcal{A}} \\ &= i|\mathbf{p}| + \frac{4\pi}{M} \frac{1}{\mathcal{A}_0} \left[ 1 - \left( \frac{\mathcal{A}_1}{\mathcal{A}_0} \right) + \left( \frac{\mathcal{A}_1^2 - \mathcal{A}_0 \mathcal{A}_2}{\mathcal{A}_0^2} \right) + \dots \right]. \end{aligned} \quad (3.19)$$

Note that to compute  $|\mathbf{p}| \cot \delta(\mathbf{p})$  to order  $\nu_0$ , one needs to compute  $\mathcal{A}_\nu$  only for  $\nu \leq \nu_0$ , which involves perturbation theory in all but the  $\nu = 0$  potential<sup>4</sup>. In the present EFT, we have found

$$\mathcal{A}_0 = \frac{C}{1 + iCM|\mathbf{p}|/4\pi} = \frac{4\pi/M}{-1/a - i|\mathbf{p}|} \quad (3.20)$$

(from eqs. (3.5), (3.15)),  $\mathcal{A}_1 = 0$ , and

$$\begin{aligned} \mathcal{A}_2 &= - \left( \frac{C}{1 + iCM|\mathbf{p}|/4\pi} \right)^2 \left( \frac{\mathbf{p}^2}{C\Lambda^2} \right) \\ &= - \left( \frac{M\mathcal{A}_0^2}{4\pi} \right) \left( \frac{1}{2} r_0 \mathbf{p}^2 \right), \end{aligned} \quad (3.21)$$

obtained by expanding eq. (3.13) to first order in  $1/\Lambda^2$  and substituting the values (3.15). Substituting the above expressions into eq. (3.19), we find that the  $\nu = 2$  expansion of

---

<sup>4</sup> In a theory with just nucleons, all  $\mathcal{A}_\nu$  vanish for odd  $\nu$ ; this is no longer true when pions are included.

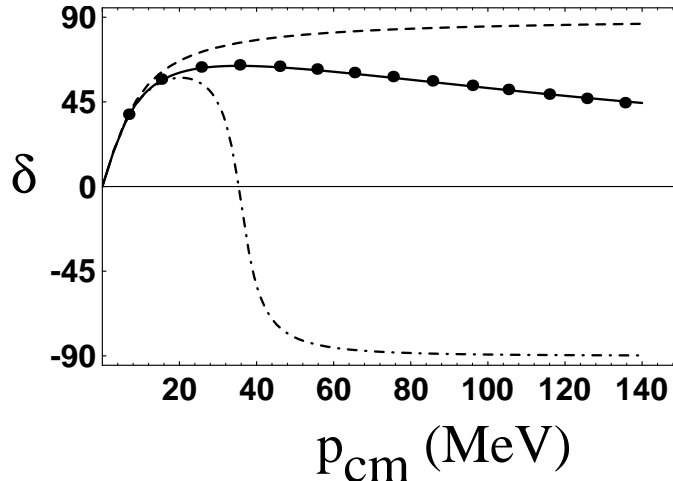


Fig. 3.  $^1S_0$   $np$  phase shifts in degrees plotted versus center of mass momentum. The dots are the  $^1S_0$  phase shift data from the Nijmegen partial wave analysis [17]; the dashed, dash-dot and solid lines are EFT calculations in a theory without pions. The dashed line is the  $\nu = 0$  result from eq. (3.11); the dash-dot line is the EFT result when the potential is expanded to order  $\nu = 2$ , eq. (3.16); the solid line (which lies along the dots) is the EFT result when  $|\mathbf{p}| \cot \delta(\mathbf{p})$  is expanded to order  $\nu = 2$ , eq. (3.22).

$|\mathbf{p}| \cot \delta(\mathbf{p})$  exactly reproduces effective range theory,

$$|\mathbf{p}| \cot \delta(\mathbf{p}) = -\frac{1}{a} + \frac{1}{2}r_0\mathbf{p}^2 \quad (\nu = 2) . \quad (3.22)$$

In fact, with no long range interactions, effective range theory had to be equivalent to the  $\nu = 2$  EFT expansion of  $|\mathbf{p}| \cot \delta(\mathbf{p})$ , by dimensional analysis. However, when pions are included the EFT expansion of  $|\mathbf{p}| \cot \delta(\mathbf{p})$  is *not* equivalent to effective range theory, since each order in the  $\nu$  expansion generates a complicated dependence for  $|\mathbf{p}| \cot \delta(\mathbf{p})$  on  $\mathbf{p}$  and  $m_\pi$  of order  $Q^\nu$ . In fact, as we show in the next section where we include pions, the lowest order,  $\nu = 0$  calculation (with the scattering length  $a$  as experimental input) allows us to predict a nonzero value for the  $^1S_0$  effective range  $r_0$ .

#### 3.4. Comparison with data

In fig. 3 we show a plot of the  $^1S_0$   $NN$  phase shift produced by the Nijmegen partial wave analysis [17], compared with the three EFT analyses we have performed without pions: the  $\nu = 0$  calculation (3.11); the  $\mu = 2$  expansion of the kernel  $V$  (3.16); and the



$\nu = 2$  expansion of  $|\mathbf{p}| \cot \delta(\mathbf{p})$  (3.22). The first two calculations yield results that agree well with data for  $|\mathbf{p}| \lesssim 20$  MeV, but differ wildly above that scale. This is what one would expect from the size of  $C$  and  $\Lambda^2$  in eqs. (3.9), (3.15). In contrast, the  $\nu = 2$  expansion of  $|\mathbf{p}| \cot \delta(\mathbf{p})$  yields a result indistinguishable from the Nijmegen analysis beyond  $|\mathbf{p}| = m_\pi$ . This demonstrates the nearly complete cancellation between operators of different index  $\mu$  discussed above, at momenta greater than  $\Lambda$ .

We do not wish to belabor this phenomenological success with this simplistic model — we have only shown that low energy EFT can reproduce effective range theory, and we have only considered a single partial wave. However, we have demonstrated that expansion of  $|\mathbf{p}| \cot \delta(\mathbf{p})$  extends the range of validity of the EFT beyond the scale set by the derivative expansion<sup>5</sup>. There is also an important practical reason for preferring to expand  $|\mathbf{p}| \cot \delta(\mathbf{p})$ : that is that the effects of  $\mu > 0$  interactions need only be computed in perturbation theory, following the expansion (3.19). This in general leads to a great simplification of the calculation. Furthermore, it provides a way to implement a consistent renormalization procedure, as we will see in the next section, where we introduce pions.

### 3.5. Rethinking the EFT expansion

We showed above that the effective Lagrangian is a momentum expansion in powers of  $p^2 ar_0$ , where  $r_0$  is a typical hadronic scale (*i.e.*  $\sim 1$  fermi), while  $a$  is the scattering length. This led us to the conclusion that the object with a sensible momentum expansion is not the potential, but rather  $\text{Re}[1/\mathcal{A}]$ , the real part of the inverse Feynman amplitude. Another conclusion we can draw is that the power counting scheme presented in §2 needs modification — eq. (2.2) in particular. The leading, 4-fermion operator has a coefficient  $4\pi a/M$ , and is treated as a  $\mu = 0$  contribution to the potential. Since the combination  $MQ$  is assumed to be of degree  $\nu = 0$ , it follows that powers of  $aQ$  appearing in the amplitude are also of degree  $\nu = 0$ . As the effective Lagrangian is an expansion in  $\sim \mathbf{p}^2 ar_0$ , a  $2d$  derivative vertex does not contribute  $\mu = 2d$  to a graph, as assumed in eq. (2.2), but rather  $\mu = d$  as it scales like  $(aQ^2)^d$ . This does not matter in the present theory; the

---

<sup>5</sup> This suggests that the EFT might be profitably formulated with a light degree of freedom in the  $s$ -channel.

“ $\nu = 2$  calculation” needs only to be renamed the “ $\nu = 1$  calculation”. However as we show below, there are striking implications when pions are included in the EFT.

#### 4. The effective theory with nucleons and pions

In order to extend the energy range over which the effective theory is useful, it is necessary to include more light degrees of freedom. The obvious candidate to add to the theory is the pion. In the previous section, analyzing  $np$  scattering in an effective theory without pions, we found that the derivative expansion in the EFT broke down at a scale  $\Lambda \simeq 35$  MeV. A sign that we are improving the utility of the EFT by including pions will be whether or not the scale set by the contact interactions becomes significantly higher. As we will show, that is the case.

Chiral symmetry mandates that pions couple to nucleons derivatively, or proportional to powers of the quark masses. In the power counting arguments of §2, we assumed  $Q^2 \sim m_\pi^2 \propto m_q$ , where  $m_q$  are the  $u$  and  $d$  quark masses. To determine which operators to include at a given order in the EFT expansion, it is necessary to look to eqs. (2.2) and (2.3). To compute the 2-nucleon potential at order  $\mu = 0$  we include all tree level interactions for which  $\sum V_i(d_i + \frac{1}{2}n_i - 2) = 0$ . That includes the 4-nucleon interaction without derivatives, as well as 1-pion exchange with the 1-derivative axial vector coupling at each vertex. In this section we perform the leading ( $\nu = 0$ ) and subleading ( $\nu = 1$ ) calculations exactly.

##### 4.1. The $\nu = 0$ amplitude

The  $\mu = 0$ , 2-nucleon potential  $V_0$  for  $NN$  scattering in the  $^1S_0$  channel is given to leading order by one pion exchange, plus a contact term:

$$V(\mathbf{p}, \mathbf{p}') = C - \left( \frac{g_A^2}{2f_\pi^2} \right) \frac{(\mathbf{q} \cdot \sigma_1 \mathbf{q} \cdot \sigma_2)(\tau_1 \cdot \tau_2)}{(\mathbf{q}^2 + m_\pi^2)}, \quad (4.1)$$

with  $\mathbf{q} \equiv (\mathbf{p} - \mathbf{p}')$ . The coupling  $g_A = 1.25$  is the axial coupling constant,  $m_\pi = 140$  MeV is the pion mass, and  $f_\pi$  is the pion decay constant normalized to be

$$f_\pi = 132 \text{ MeV}, \quad (4.2)$$

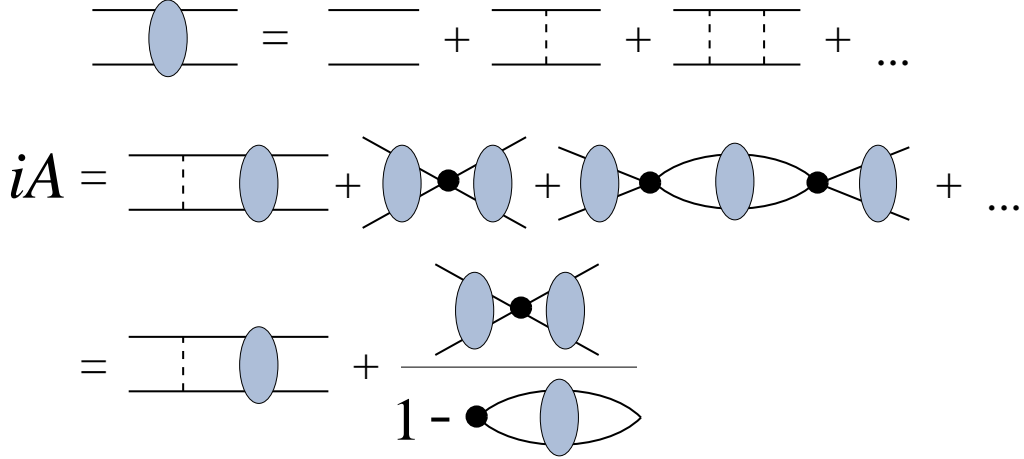


Fig. 4. Ladder diagrams for the  $\nu = 0$  contribution to the Feynman amplitude  $\mathcal{A}_0$  are formally resummed by expressing the kernel  $V_0$  as a sum of a contact interaction proportional to  $\tilde{C}$  and a nonlocal interaction  $V_\pi$  as in eq. (4.3). The shaded blobs consist of the ladder sum of  $V_\pi$  interactions (dashed lines), while the black vertices correspond to a factor of  $\tilde{C}$ .

compared to other common normalizations  $f_\pi = \sqrt{2}(93 \text{ MeV}) = (186 \text{ MeV})/\sqrt{2}$ . As in the previous section,  $C$  is a free parameter which will be computed in  $\overline{MS}$  subject to the condition that we correctly reproduce the measured threshold scattering amplitude (*i.e.*, the scattering length  $a$ ). Since we are exclusively interested in the  $^1S_0$  channel ( $I = 1$ ) we can express  $V_0$  as

$$V_0(\mathbf{p}, \mathbf{p}') = \tilde{C} + V_\pi(\mathbf{p}, \mathbf{p}') , \quad (4.3)$$

where

$$\tilde{C} \equiv \left( C + \frac{g_A^2}{2f_\pi^2} \right) , \quad V_\pi(\mathbf{p}, \mathbf{p}') \equiv -\frac{4\pi\alpha_\pi}{(\mathbf{q}^2 + m_\pi^2)} , \quad \alpha_\pi \equiv \left( \frac{g_A^2 m_\pi^2}{8\pi f_\pi^2} \right) . \quad (4.4)$$

Note that while  $V_\pi$  is the conventional one-pion exchange (OPE) potential, our calculation will differ significantly from OPE due to the  $\tilde{C}$  contact interaction. The contact term includes not only the  $\delta^3(\mathbf{r})$  contribution from one pion exchange, but also the leading contribution in the derivative expansion of all shorter distance effects, such as 2-pion exchange, intermediate  $\Delta$ 's,  $\omega$  exchange, etc.

It is not possible to compute the ladder sum with the above kernel analytically, but we are able to express it in terms of several quantities that can be computed numerically

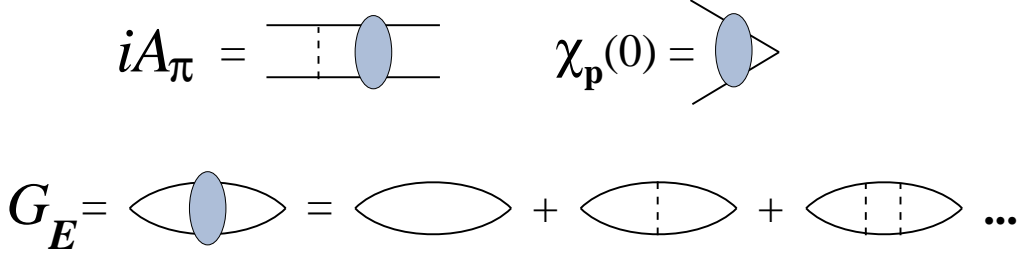


Fig. 5. Subdiagrams defining the quantities  $\mathcal{A}_\pi$ ,  $\chi_{\mathbf{p}}(\mathbf{0})$  and  $\tilde{G}_E(\mathbf{0}, \mathbf{0})$  used in eq. (4.5).  $\mathcal{A}_\pi$  and  $\chi_{\mathbf{p}}(\mathbf{0})$  are finite, as are all but the first two diagrams in the expansion of  $\tilde{G}_E(\mathbf{0}, \mathbf{0})$ . The shaded blob is defined diagrammatically in fig. 4. Dashed lines are insertions of  $V_\pi$ , eq. (4.4)

with ease. Most importantly, we are able to renormalize the nonperturbative amplitude analytically. To achieve this, the ladder diagrams are formally summed as in fig. 4 to yield the Feynman amplitude<sup>6</sup>

$$i\mathcal{A}_0 = i\mathcal{A}_\pi - i \frac{\tilde{C} [\chi_{\mathbf{p}}(\mathbf{0})]^2}{1 - \tilde{C}\tilde{G}_E(\mathbf{0}, \mathbf{0})}, \quad (4.5)$$

where the quantities  $\mathcal{A}_\pi$ ,  $\chi_{\mathbf{p}}(\mathbf{0})$  and  $\tilde{G}_E(\mathbf{0}, \mathbf{0})$  are the sub-diagrams pictured in fig. 5.

The quantity  $\mathcal{A}_\pi$  is just the amplitude one finds in the pure Yukawa theory with potential  $\hat{V}_\pi$ , i.e, the usual OPE result:

$$\begin{aligned} i\mathcal{A}_\pi &= \langle \mathbf{p} | \hat{V}_\pi (1 + \hat{G}_E \hat{V}_\pi) | \mathbf{p}' \rangle, \\ \hat{G}_E &= \frac{1}{E - \hat{H}_0 - \hat{V}_\pi + i\epsilon}, \end{aligned} \quad (4.6)$$

while

$$\chi_{\mathbf{p}}(\mathbf{0}) = \int \frac{d^3\mathbf{q}}{(2\pi)^3} \langle \mathbf{q} | (1 + \hat{G}_E \hat{V}_\pi) | \mathbf{p} \rangle \quad (4.7)$$

is the OPE wave function at the origin. Both  $\mathcal{A}_\pi$  and  $\chi_{\mathbf{p}}(\mathbf{0})$  can be computed numerically by solving the Schrödinger equation with the Yukawa potential  $V_\pi$ . This is discussed in appendix A, where the solutions are plotted (figs. 7,8).

The quantity  $\tilde{G}_E(\mathbf{0}, \mathbf{0})$  is the coordinate-space propagator from the origin to the origin in the presence of  $V_\pi$ ; it is divergent but can be defined in  $\overline{MS}$

$$\tilde{G}_E(\mathbf{0}, \mathbf{0}) = \iint \frac{d^3\mathbf{q}}{(2\pi)^3} \frac{d^3\mathbf{q}'}{(2\pi)^3} \langle \mathbf{q}' | \hat{G}_E | \mathbf{q} \rangle. \quad (4.8)$$

---

<sup>6</sup> Here we give a Feynman diagram approach, while in appendix A we show how the Schrödinger equation corresponding to the kernel (4.1) can be solved directly.

Divergences occur in only the first two graphs in the perturbative expansion for  $\tilde{G}_E(\mathbf{0}, \mathbf{0})$  shown in fig 5. These two graphs can be computed in  $\overline{MS}$ , while the remaining graphs can be summed by numerically computing the propagator  $\tilde{G}_E(\mathbf{r}, \mathbf{0})$ ; see appendix A for details. As a result of renormalization,  $\tilde{G}_E(\mathbf{0}, \mathbf{0})$  is replaced by the finite  $\tilde{G}_E^{\overline{MS}}(\mathbf{0}, \mathbf{0})$ , while the bare  $\tilde{C}$  is replaced by the renormalized  $\tilde{C}_{\overline{MS}}(\mu)$  which is to be fit to experiment. Note that both quantities now depend on a renormalization scale  $\mu$ ; however the amplitude  $\mathcal{A}_0$  is  $\mu$  independent. We can compute the renormalization group equation for  $\tilde{C}_{\overline{MS}}(\mu)$ , which is given by

$$\mu \frac{\partial}{\partial \mu} \frac{1}{\tilde{C}_{\overline{MS}}(\mu)} = -\frac{\alpha_\pi M^2}{4\pi} \quad (\overline{MS}) . \quad (4.9)$$

This result is derived in appendix A (see eq. (A.28)). Throughout this paper we will be quoting values for coupling constants renormalized at the scale  $\mu = m_\pi$ ; the reason for this is that loop diagrams omitted at a given level of the  $\nu$  expansion bring in factors of  $\ln m_\pi^2/\mu^2$ , and so choosing  $\mu \sim m_\pi$  is expected to optimize the perturbation expansion for  $|\mathbf{p}| \lesssim m_\pi$ . Note that for  $\tilde{C}_{\overline{MS}}(\mu)$  negative,  $|1/\tilde{C}_{\overline{MS}}(\mu)|$  increases with increasing renormalization scale  $\mu$ .

After solving for  $\mathcal{A}_\pi$ ,  $\chi_{\mathbf{p}}$  and  $G_E^{\overline{MS}}$  numerically, one can compute the amplitude (4.5) and fit  $C_{\overline{MS}}(\mu)$  in order to obtain the correct scattering length. We find

$$C_{\overline{MS}}(\mu) \Big|_{\mu=m_\pi} = -\left(\frac{1}{79 \text{ MeV}}\right)^2 \quad (\nu = 0) , \quad (4.10)$$

( $C_{\overline{MS}} \equiv \tilde{C}_{\overline{MS}} - g_A^2/2f_\pi^2$ ) which shows a substantial improvement over the value  $C = -(1/25 \text{ MeV})^2$  obtained in the pure nucleon effective theory at  $\nu = 0$ , eq. (3.9). Furthermore, once  $C_{\overline{MS}}$  is fixed to give the correct scattering length, one can compute the effective range, and we find

$$r_0 = 1.3 \text{ fm} \quad (\nu = 0) , \quad (4.11)$$

which shows that this simple effective theory with a contact term and one-pion exchange can account for about half of the measured effective range,  $r_0 = 2.7 \text{ fm}$ . In fig. 7 we plot the phase shift determined from the amplitude  $\mathcal{A}_0$  in eq. (4.5) as a function of the center of mass momentum  $|\mathbf{p}|$ .

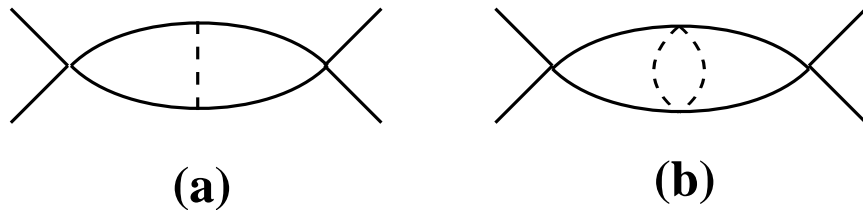


Fig. 6. Examples of graphs with logarithmic divergences: (a) one proportional to  $M^2 m_\pi^2$ ; (b) another with a term proportional to  $M^2 \mathbf{p}^4$ . The solid lines are nucleons, while the dashed lines are pions.

#### 4.2. A new power counting scheme

In section §3.5 we pointed at that the parametrically large coefficients of operators in the effective Lagrangian forced us to revise our power counting scheme; however the revised counting had little practical effect in the theory without pions. However, with pions the story is different. In particular, equation (4.9) above mandates that we modify our EFT expansion scheme significantly. The logarithmically divergent graph that leads to the scaling of  $C$  is shown in fig. 6(a); in  $4 - 2\epsilon$  dimensions it gives rise to the pole

$$-\frac{1}{\epsilon} \frac{\alpha_\pi M^2}{16\pi} = -\frac{1}{\epsilon} \frac{g_A^2 m_\pi^2 M^2}{128\pi^2 f_\pi^2}. \quad (4.12)$$

By our power counting, it is perfectly consistent to find such a divergence at  $\nu = 0$ , since  $m_\pi^2 M^2$  has degree  $\nu = 0$ . However, note that the counterterm required to absorb this divergence is of the form  $(N^\dagger \mathcal{M}_q N)(N^\dagger N)$ , where  $\mathcal{M}_q$  is the quark mass matrix. In the power counting scheme described in §2, such an operator, which is higher order in a chiral expansion, was considered to be a  $\mu = 2$  operator, since it was assumed that the coefficient of the operator was set by a “typical” QCD scale. Instead, we see from eq. (4.12) that the coefficient of this operator has an explicit factor of  $M^2$ , and so is actually of degree  $\mu = 0$ <sup>7</sup>.

---

<sup>7</sup> The connection between the coefficient of a  $1/\epsilon$  pole, and the natural size of the coefficients of operators in the effective Lagrangian is “naive dimensional analysis”. The idea is simply that, because of the RG flow such as in eq. (4.9), even if the coefficient  $C(\mu)$  of an operator is small for some reason at a scale  $\mu_0$ , at a scale  $\mu = \mu_0 \times \mathcal{O}(1)$ ,  $C(\mu)$  will have flowed to the magnitude of the coefficient of the  $1/\epsilon$  pole, which is therefore considered its “natural” size.

Evidently the EFT expansion is *not* equivalent to a chiral expansion in  $m_\pi$ , since a calculation at finite order in the EFT expansion can be modified by arbitrary powers of  $M^2 m_\pi^2$ . This may sound like a disaster for the EFT expansion, but it actually is not. At  $\nu = 0$ , for example, we still have only one contact interaction  $C$ , and whether or not this contains contributions from all orders in  $m_\pi$  has no effect on the predictive power of the calculation.

What would be a disaster is if there were counterterms needed proportional to powers of  $M^2 \mathbf{p}^2$ . If that were the case, the theory would not be predictive, as an entire form factor would be needed to describe scattering at lowest order in the EFT expansion. However such terms do not arise. Consider the diagram fig. 6(b), which contributes to the  $\nu = 2$  calculation of the amplitude. The graph is proportional to  $C^2 M^2 / f^4 \sim 1/(\text{mass})^6$ . Since the graph must be proportional to  $1/(\text{mass})^2$ , there can be a logarithmic divergence (and hence a  $1/\epsilon$  pole that requires a counterterm) proportional to  $C^2 M^2 \mathbf{p}^4 / f^4$ . This is consistent with the graph being  $\nu = 2$ ; it is also consistent with the power counting of the theory without pions, where the  $\mathbf{p}^4$  interaction was multiplied by  $(ar_0)^2$ . However, this result is not consistent with the naive power counting in §2 that assigned degree  $\mu = 4$  to a four nucleon contact interaction proportional to  $\mathbf{p}^4$ .

It is possible to make general power counting arguments that the four nucleon contact terms in the effective Lagrangian involve an expansion in  $M^2 m_\pi^2$  and  $M \mathbf{p}^2$ . Equation (2.2) is therefore modified so that the degree  $\mu$  of a vertex gets a contribution  $\Delta\mu = 1$  rather than  $\Delta\mu = 2$  from each factor of nucleon momentum squared,  $\mathbf{p}^2$ . Furthermore, powers of  $\mathcal{M}_q$  in four nucleon contact interactions are assumed to be accompanied by  $M^2$  and do not increase  $\mu$ .

#### 4.3. The full $\nu = 1$ amplitude with one-pion exchange

From the above discussion we see that the  $\mathbf{p}^2$  contact interaction — given that its coefficient scales  $\sim M$  — is the only operator in the effective Lagrangian of degree  $\mu = 1$ . Two pion exchange — considered of equal order in the incorrect power counting of §2 — contributes at order  $\mu = 2$ , as does the  $\mathbf{p}^4$  contact interaction. A full  $\nu = 1$  treatment of the  $^1S_0$  scattering amplitude is therefore simple to obtain, while extending the analysis to

$\nu = 2$  is quite ambitious.

As in §3, we first consider the Weinberg expansion, summing up the  $\mu = 1$  potential  $V = V_0 + V_1$  to all orders, where  $V_0$  is given in eq. (4.3) and

$$V_1 = \tilde{C} \left( \frac{\mathbf{p}^2 + \mathbf{p}'^2}{2\Lambda^2} \right). \quad (4.13)$$

The resultant amplitude is (see appendix B for details)

$$i\mathcal{A}_{V_1} = i\mathcal{A}_\pi - i \frac{[\chi_{\mathbf{p}}(\mathbf{0})]^2}{\left[ \tilde{C} \left( 1 - \alpha_\pi m_\pi M / \Lambda^2 + \mathbf{p}^2 / \Lambda^2 \right) \right]^{-1} - \tilde{G}_E(\mathbf{0}, \mathbf{0})}, \quad (4.14)$$

where  $\mathcal{A}_\pi$ ,  $\chi_{\mathbf{p}}(\mathbf{0})$  and  $\tilde{G}_E(\mathbf{0}, \mathbf{0})$  are defined as in the previous section, fig. 5. Expanding the denominator of eq. (4.7) in powers of  $1/\Lambda^2$  gives

$$\frac{1}{\tilde{C}} + \frac{1}{\tilde{C}} \left( \frac{\alpha_\pi m_\pi M}{\Lambda^2} + \frac{\mathbf{p}^2}{\Lambda^2} \right) + \dots - \tilde{G}_E(\mathbf{0}, \mathbf{0}). \quad (4.15)$$

The term  $\tilde{G}_E$  is divergent and if it is defined using dimensional regularization it has an energy independent  $1/\epsilon$  singularity. Using the  $\overline{MS}$  subtraction scheme, this divergence is absorbed into a renormalization of  $\tilde{C}$  changing it to  $\tilde{C}_{\overline{MS}}(\mu)$ . Then in the second term proportional to  $1/\Lambda^2$  we must introduce a renormalized  $\Lambda_{\overline{MS}}(\mu)$  defined by  $\tilde{C}\Lambda^2 = \tilde{C}_{\overline{MS}}(\mu)\Lambda_{\overline{MS}}(\mu)^2$ . However, with  $\tilde{C}$  and  $\Lambda$  renormalized in this way there is no freedom to express the higher order terms represented by the ellipses in eq. (4.15) in terms of renormalized parameters. This problem arises because we have not included operators with more than two derivatives. They are needed as counter terms to render multiple insertions of the two derivative operator in eq. (3.1) finite. This is equivalent to saying that no redefinition of couplings in eq. (4.14) can absorb the energy independent  $1/\epsilon$  pole in  $\tilde{G}_E(\mathbf{0}, \mathbf{0})$ .

A procedure which we can follow, consistent to order  $\nu = 1$  in an expansion of the amplitude, is to include all the higher derivative operators, absorb the  $1/\epsilon$ , and then arbitrarily set the renormalized coefficients of the higher order terms to zero. This *ad hoc* procedure results in the analog of eq. (3.13), with one pion exchange effects included:

$$i\mathcal{A}_{V_1} = i\mathcal{A}_\pi - i \frac{[\chi_{\mathbf{p}}(\mathbf{0})]^2}{\left[ \tilde{C}_{\overline{MS}} \left( 1 - \alpha_\pi m_\pi M / \Lambda_{\overline{MS}}^2 + \mathbf{p}^2 / \Lambda_{\overline{MS}}^2 \right) \right]^{-1} - \tilde{G}_E^{\overline{MS}}(\mathbf{0}, \mathbf{0})}. \quad (4.16)$$



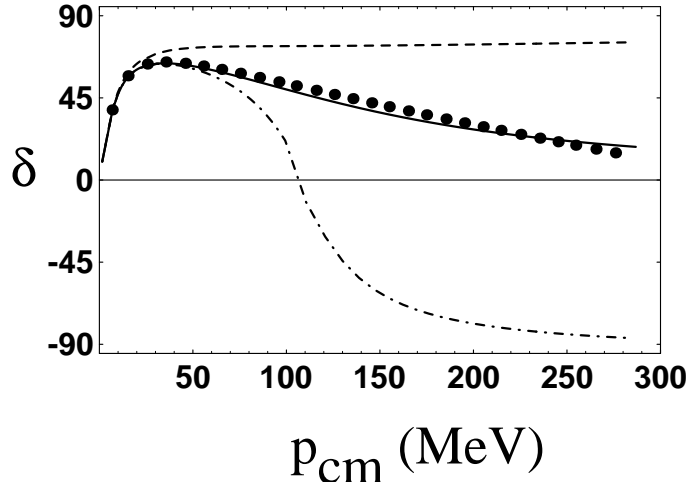


Fig. 7.  $^1S_0$   $np$  phase shifts in degrees plotted versus center of mass momentum. The dots are the  $^1S_0$  phase shift data from the Nijmegen partial wave analysis [17]; the dashed, dash-dot and solid lines are EFT calculations in a theory with one pion exchange. The dashed line is the  $\nu = 0$  result from eq. (4.5); the dash-dot line is the EFT result when the potential is expanded to order  $\nu = 1$ , eq. (4.14); the solid line (which lies along the dots) is the EFT result when  $|\mathbf{p}| \cot \delta(\mathbf{p})$  is expanded to order  $\nu = 1$ , eqs. (4.18)–(4.20). Note that the momentum range of the plot extends to  $2m_\pi$ , twice the range of fig. 3.

A (numerical) fit to the measured scattering length and effective range with the amplitude in eq. (4.16) gives

$$C_{MS}(\mu) \Big|_{\mu=m_\pi} = -\frac{1}{(125 \text{ MeV})^2}, \quad \frac{\Lambda_{MS}^2(\mu)}{\Lambda_{MS}^2} \Big|_{\mu=m_\pi} = -\frac{1}{(43 \text{ MeV})^2}. \quad (4.17)$$

Comparing the above values with the analogue without pions, eq. (3.15), we see that the inclusion of pions has greatly reduced the value of  $C$ , while not significantly altering the scale  $\Lambda$  of the derivative expansion. Therefore, the range of utility of the EFT apparently remains disappointingly small. In particular, the scale  $\Lambda$  is far below the Fermi momentum in nuclear matter ( $p_F \sim 280$  MeV) so that the theory would appear to be of little utility in understanding nuclear physics. Nevertheless, following the discussion in §3.3, we expect an expansion of  $|\mathbf{p}| \cot \delta(\mathbf{p})$  to order  $\nu = 1$  will work much better; this is indeed the case, as demonstrated in fig. 7.

To compute the  $\nu = 1$  expansion of  $|\mathbf{p}| \cot \delta(\mathbf{p})$  we need to know  $\mathcal{A}_0$  and  $\mathcal{A}_1$ . The amplitude  $\mathcal{A}_0$  was computed in the previous section in eq. (4.5), with the substitution of

the  $\overline{MS}$  values for  $\tilde{C}$  and  $\tilde{G}_E$ :

$$\mathcal{A}_0 = \mathcal{A}_\pi - \frac{[\chi_{\mathbf{p}}(\mathbf{0})]^2}{1/\tilde{C}_{\overline{MS}} - \tilde{G}_E^{\overline{MS}}(\mathbf{0}, \mathbf{0})} . \quad (4.18)$$

The second order amplitude  $\mathcal{A}_1$  corresponds to the sum of graphs indicated in fig. 2; their sum is given by our previous calculation (4.16) expanded to first order in  $1/\Lambda^2$ :

$$\mathcal{A}_1 = \frac{[\chi_{\mathbf{p}}(\mathbf{0})]^2}{\tilde{C}_{\overline{MS}} \left[1/\tilde{C}_{\overline{MS}} - \tilde{G}_E^{\overline{MS}}(\mathbf{0}, \mathbf{0})\right]^2} \left( \alpha_\pi m_\pi M / \Lambda_{\overline{MS}}^2 - \mathbf{p}^2 / \Lambda_{\overline{MS}}^2 \right) . \quad (4.19)$$

The  $\nu = 1$  expansion of  $|\mathbf{p}| \cot \delta(\mathbf{p})$  is given by eq. (3.19):

$$|\mathbf{p}| \cot \delta(\mathbf{p}) = i|\mathbf{p}| + \frac{4\pi}{M} \frac{1}{\mathcal{A}_0} \left[ 1 - \left( \frac{\mathcal{A}_1}{\mathcal{A}_0} \right) \right] \quad (\nu = 1) . \quad (4.20)$$

This procedure is well defined from the point of view of renormalization: Note that aside from the explicit factor of  $\mathbf{p}^2$  in eq. (4.19), there is also complicated momentum dependence in  $\mathcal{A}_\pi$ ,  $\chi_{\mathbf{p}}(\mathbf{0})$  and  $\tilde{G}_E^{\overline{MS}}$  (OPE Feynman amplitude, the OPE wave function at the origin, the renormalized OPE Green function at the origin respectively). Thus the terms in the expansion (4.20) do not correspond to the two parameters in effective range theory; indeed, we saw in the previous section that the  $\nu = 0$  contribution already accounts for half of the effective range.

By fitting the two free parameters  $\tilde{C}_{\overline{MS}}$  and  $\Lambda_{\overline{MS}}^2$  so that the expression (4.20) correctly reproduces the  $^1S_0$  effective range and scattering length, we arrive at the prediction for the phase shift plotted as a solid line in fig. 7. The values one finds for the parameters are now:

$$C_{\overline{MS}}(\mu) \Big|_{\mu=m_\pi} = -\frac{1}{(100 \text{ MeV})^2} , \quad \frac{1}{\Lambda_{\overline{MS}}^2(\mu)} \Big|_{\mu=m_\pi} = -\frac{1}{(121 \text{ MeV})^2} , \quad (4.21)$$

which indicates a very significant improvement over those found by first expanding the potential to order  $\mu = 1$  and then summing to all orders, eq. (4.17). In particular, the momentum expansion scale  $\Lambda$  is now much larger.

Even with the larger scale  $|\Lambda| = 121 \text{ MeV}$ , one would not expect the momentum expansion to converge fast enough to be of use in nuclear matter, where  $p_F \sim 280 \text{ MeV}$ . However, as argued in the previous section and evidenced by fig. 7, the expansion for  $|\mathbf{p}| \cot \delta(\mathbf{p})$  has a much larger radius of convergence than the derivative expansion in the Lagrangian.

## 5. Conclusions

We have shown how to perform a nonperturbative calculation of  $NN$  scattering in the  $^1S_0$  channel in an effective field theory expansion. A key feature of the procedure was the application of dimensional regularization (usually viewed as a perturbative regulator) and the  $\overline{MS}$  renormalization scheme procedure to the nonperturbative problem. Our results for the phase shift depend only on physical observables and not on any momentum cutoff, even though the bare  $NN$  interactions in an EFT are singular.

At leading order in the EFT expansion ( $\nu = 0$ ), which includes one pion exchange and a contact interaction, we find a prediction for the effective range  $r_0 = 1.3$  fm, given the measured scattering length; this is about half the measured value. The fit to the measured phase shift is poor above  $|\mathbf{p}| \sim 25$  MeV. In order to better understand the range of validity of the EFT approach, we investigated the phase shift including effects at subleading order in the EFT expansion. At this order there is an ambiguity about what quantity should be expanded; the ambiguity corresponds to which higher order terms are kept in the EFT expansion to maintain unitarity. Following the method of [3], one can expand the potential to subleading order in the EFT expansion, and include its effects to all orders. Doing this, we find the phase shift that results disagrees with data above  $|\mathbf{p}| \sim 45$  MeV, which is what one expects from the size of coefficients one finds for the derivative expansion of the effective Lagrangian.

An alternative method we explore is to expand the quantity  $|\mathbf{p}| \cot \delta(\mathbf{p})$  to subleading order. We explain why this expansion should be expected to have a greater radius of convergence than the derivative expansion would lead one to expect, at least at low orders in the EFT expansion. This is supported by calculation, which suggests that the  $^1S_0$  phase shifts at subleading order agree well with data at up to  $\sim 280$  MeV. A strong correlation is implied between coefficients in the derivative expansion of the Lagrangian that has to do with an  $s$ -channel pole, but which remains to be quantitatively understood.

By investigating the EFT both with and without one pion exchange to order  $\nu = 1$ , we see that including the pion increases the inverse mass scales that appear in the EFT expansion, thereby improving its utility at high momentum. Including two pion exchange, four derivative interactions and possibly the effects of the  $\Delta$  will increase

these scales even further. Since higher partial waves are less sensitive to short distance physics (and are in fact well approximated by one pion exchange, which appears at lowest order in the EFT expansion), we are optimistic that the techniques presented here will be successful at reproducing all of the spin singlet partial wave phase shifts up to center of mass momenta comparable to the Fermi momentum in nuclear matter. This investigation is in progress.

As a consequence of our analysis we are forced to revise the power counting scheme of Weinberg [3] in order to account for the powers of the nucleon mass  $M$  that appear in operator coefficients of the effective Lagrangian. We find that the EFT expansion is not equivalent to the chiral expansion, as the EFT expansion requires summing contributions proportional to all powers of  $M^2 m_\pi^2$ .

Application of these techniques to the spin triplet channel is not straightforward, however, since the interactions in this channel are singular but not separable (*e.g.*, a  $1/r^3$  singularity from one pion exchange). Our hope is that this problem can be surmounted, in which case the techniques we developed here should prove of use in a variety of interesting problems. The EFT approach could be applied to nuclear matter, with the goal of understanding its binding energy and compressibility in terms of a few parameters extracted from low energy scattering experiments. One could investigate the implications of  $SU(4)$  symmetry in  $N$  and  $\Delta$  interactions, recently shown to be a consequence of the large- $N_c$  expansion of QCD [18] [19]. In particular,  $SU(4)$  symmetry greatly reduces the number of four-fermion operators one needs to consider when the  $\Delta$  is included [19].

Since  $SU(3)$  flavor symmetry and its breaking can be easily incorporated in the EFT formalism, it may prove a useful tool for exploring systems with nonzero strangeness, extending the discussion of ref. [10] to a nonperturbative analysis. Finally, of great interest is the possibility that the EFT analysis may prove to be a useful tool in understanding systems at densities above nuclear density, with an eye toward a systematic inclusion of nuclear forces in the presently incomplete analyses of pion condensation [20] and kaon condensation [21]–[23].

## Acknowledgements

We would like to thank G. Bertsch, A. Manohar, G. Miller, U. van Kolck, and R. Venugopalan for useful conversations and correspondence. DBK would like to acknowledge a conversation with M. Lutz on his related and independent work. MJS was supported in part by the U.S. Department of Energy under Grant No. DE-FG02-91-ER40682. DBK was supported in part by DOE grant DOE-ER-40561, and NSF Presidential Young Investigator award PHY-9057135. MBW is supported in part by the Department of Energy under Contract No. DE-FG03-92-ER40701.

## Appendix A. Solving the Schrödinger equation

In the §3 we showed how to sum ladder diagrams involving a 4-nucleon contact interaction. This is formally equivalent to solving the Schrödinger equation with a  $\delta^3(\mathbf{r})$  potential; however neither approach makes sense without renormalization. While the techniques of renormalization are familiar in the context of field theory, here we show how to obtain the same results via the Schrödinger equation (See also ref. [24]. This approach is quite convenient for practical computations.

The equation we want to solve is

$$\begin{aligned} 0 &= \left[ -\nabla^2/M + V_\pi(\mathbf{r}) + \tilde{C}\delta^3(\mathbf{r}) - E \right] \psi(\mathbf{r}) \\ &\equiv \left[ H - E + \tilde{C}\delta^3(\mathbf{r}) \right] \psi(\mathbf{r}) , \end{aligned} \tag{A.1}$$

where

$$V_\pi(\mathbf{r}) = -\alpha_\pi \frac{e^{-m_\pi r}}{r} . \tag{A.2}$$

Away from  $\mathbf{r} = 0$  we can find two independent  $s$ -wave solutions to  $(H - E)\psi = 0$ . We denote the regular  $s$ -wave solution by  $\mathcal{J}_E(r)$  and the irregular  $s$ -wave solution by  $\mathcal{K}_E^\lambda(r)$ . They are normalized to have the following behaviour near  $r = 0$ :

$$\begin{aligned} \mathcal{J}_E(r) &\xrightarrow{r \rightarrow 0} 1 - \frac{\alpha_\pi M}{2} r + \mathcal{O}(r^2) \\ \mathcal{K}_E^\lambda(r) &\xrightarrow{r \rightarrow 0} \frac{M}{4\pi r} - \frac{\alpha_\pi M^2}{4\pi} \ln \lambda r + \mathcal{O}(r \ln r) . \end{aligned} \tag{A.3}$$

These functions have several features:

(i)  $\mathcal{K}_E^\lambda$  is a Green's function satisfying

$$(H - E)\mathcal{K}_E^\lambda = \delta^3(\mathbf{r}) ;$$

(ii) The arbitrary scale  $\lambda$  in  $\mathcal{K}_E^\lambda$  corresponds to the choice of boundary conditions on the Green's function (i.e, the arbitrariness in redefining  $\mathcal{K}_E(r)$  by an amount proportional to  $\mathcal{J}_E(r)$ );

(iii) For both functions, the dependence on the energy  $E$  vanishes as  $r \rightarrow 0$ ;

(iv) asymptotically, these functions become:

$$\begin{aligned} \mathcal{J}_E(r) &\xrightarrow{r \rightarrow \infty} (ye^{ipr}/pr + c.c.) , \\ \mathcal{K}_E^\lambda(r) &\xrightarrow{r \rightarrow \infty} (ze^{ipr}/pr + c.c.) , \end{aligned} \tag{A.4}$$

where  $E = p^2/M$  and  $y$  and  $z$  are complex constants that must be determined numerically. However,  $y$  and  $z$  are related: since  $\int [\mathcal{K}_E^\lambda(H - E)\mathcal{J}_E] d^3r = 0$ , it follows upon integration by parts that

$$yz^* - y^*z = -\frac{ipM}{8\pi} . \tag{A.5}$$

The Schrödinger equation (A.1) can now be rewritten as

$$(H - E)\psi(\mathbf{r}) = -\tilde{C}\psi(\mathbf{0})\delta^3(\mathbf{r}) , \tag{A.6}$$

and is formally solved in the s-wave channel by

$$\psi(\mathbf{r}) = a\mathcal{J}_E(r) + b\mathcal{K}_E^\lambda(r) \xrightarrow{r \rightarrow \infty} (ay + bz)\frac{e^{ipr}}{pr} + c.c. \tag{A.7}$$

provided that  $b = -\tilde{C}\psi(\mathbf{0})$ , or

$$b = -a\frac{\tilde{C}}{1 + \tilde{C}\mathcal{K}_E^\lambda(0)} . \tag{A.8}$$

(We say ‘‘formally’’ since  $\mathcal{K}_E^\lambda(0)$  is divergent; we will address the issue of renormalization below). Note that the ratio  $a/b$  is real. Comparing eq. (A.7) with the desired (*s*-wave) asymptotic boundary condition

$$\psi(\mathbf{r}) \xrightarrow{r \rightarrow \infty} -\frac{i}{2} \left( e^{2i\delta} \frac{e^{ipr}}{pr} - \frac{e^{-ipr}}{pr} \right) , \tag{A.9}$$

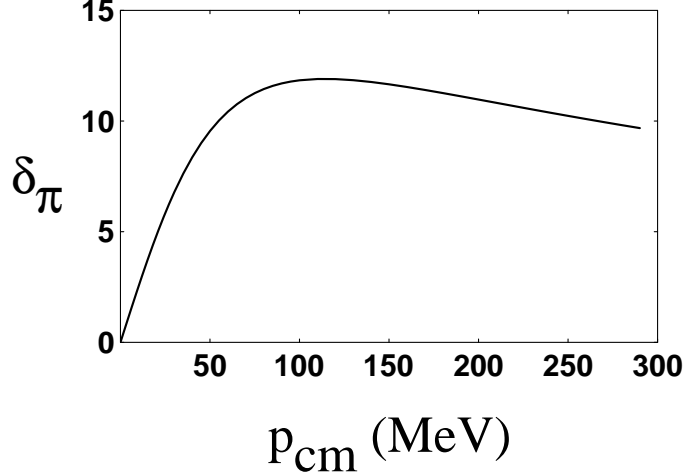


Fig. 8. The OPE phase shift  $\delta_\pi$  (in degrees) as a function of  $|\mathbf{p}|$  in MeV.

it follows that the phase shift is given by

$$\begin{aligned}
e^{2i\delta} &= -(ay + bz)/(ay + bz)^* \\
&= -\frac{y}{y^*} - \left(\frac{1}{y^*}\right)^2 \frac{zy^* - yz^*}{a/b + z^*/y^*} \\
&= e^{2i\delta_\pi} - \left(\frac{1}{y^*}\right)^2 \left(\frac{ipM}{8\pi}\right) \frac{1}{-1/\tilde{C} - \mathcal{K}_E^\lambda(0) + z^*/y^*} ,
\end{aligned} \tag{A.10}$$

where we have made use of eqs. (A.5), (A.8), and have defined  $\delta_\pi$  to be the ‘‘OPE’’ s-wave phase shift arising from the one pion exchange Yukawa interaction  $V_\pi$ , and no contact term ( $\exp(2i\delta_\pi) = -y/y^*$ ) (see fig. 8) <sup>8</sup>.

It is now just a few steps to relate the above expression to eq. (4.5), the analogous formula derived diagrammatically. First note that the canonically normalized scattering solution in the pure Yukawa theory is given by  $\chi_{\mathbf{p}}(\mathbf{r}) = -i\mathcal{J}_E(r)/(2y^*)$ , so that

$$\chi_{\mathbf{p}}(\mathbf{0}) = -i/(2y^*) . \tag{A.11}$$

The function  $[\chi_{\mathbf{p}}(\mathbf{0})]^2$  is plotted in fig. 9 as a function of the centre-of-mass momentum.

Next note that the retarded Green’s function (satisfying the asymptotic boundary condition that there is no incoming wave) is given by

$$\tilde{G}_E(\mathbf{r}, \mathbf{0}) = (-\mathcal{K}_E^\lambda(r) + (z^*/y^*)\mathcal{J}_E(r)) ; \tag{A.12}$$

---

<sup>8</sup> Our numerical calculations were performed with  $m_\pi = 140$  MeV and  $M = 940$  MeV.

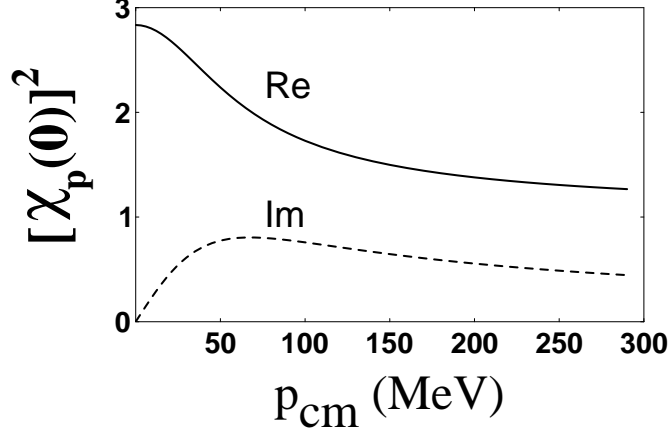


Fig. 9. The OPE wave function squared at the origin,  $[\chi_{\mathbf{p}}(\mathbf{0})]^2$ , plotted versus momentum in MeV. The solid and dashed lines correspond to the real and imaginary parts respectively.

finally, the relation between the Feynman amplitude  $i\mathcal{A}$  and the phase shift is

$$i\mathcal{A} = i \frac{4\pi(e^{2i\delta} - 1)}{2ipM}. \quad (\text{A.13})$$

It follows that expression (A.10) is equivalent to eq. (4.5):

$$i\mathcal{A} = i\mathcal{A}_\pi - i \frac{\tilde{C} [\chi_{\mathbf{p}}(\mathbf{0})]^2}{1 - \tilde{C}\tilde{G}_E(\mathbf{0}, \mathbf{0})}. \quad (\text{A.14})$$

When the effects of pions are not included, as in §3, one recovers the amplitude (3.10), since  $\alpha_\pi \rightarrow 0$  implies  $\mathcal{A}_\pi \rightarrow 0$ ,  $\tilde{C} \rightarrow C$ ,  $\chi_{\mathbf{p}}(\mathbf{0}) \rightarrow 1$ , and  $G_E \rightarrow G_E^0$  in the above expression.

So far the discussion has been in terms of the quantity,  $\mathcal{K}_E^\lambda(0)$ , which was seen in eq. (A.3) to have both linear and logarithmic divergences as  $r \rightarrow 0$ . This can be remedied by renormalizing  $\tilde{C}$ , for example by defining

$$\frac{1}{\tilde{C}_R(\lambda)} \equiv \frac{1}{\tilde{C}} + \mathcal{K}_0^\lambda(0) = \frac{1}{\tilde{C}} + \mathcal{K}_E^\lambda(0), \quad (\text{A.15})$$

(where we used the fact that  $\lim_{r \rightarrow 0} [\mathcal{K}_E^\lambda(r) - \mathcal{K}_0^\lambda(r)] = 0$ , from eq. (A.3)). Then eq. (A.10) for the phase shift can be written in terms of renormalized quantities as

$$e^{2i\delta} = e^{2i\delta_\pi} - \left(\frac{1}{y^*}\right)^2 \left(\frac{ipM}{8\pi}\right) \frac{1}{-1/\tilde{C}_R(\lambda) + z^*/y^*}. \quad (\text{A.16})$$



This choice of renormalization scheme is convenient for computations: First one solves for the solutions to the Schrödinger equation with the OPE potential  $V_\pi(\mathbf{r})$ , subject to the boundary condition (A.3); from that one computes the asymptotic behaviour and the coefficients  $y$  and  $z$  in eq. (A.4); then one computes  $C_R(\lambda)$  from eq. (A.16) in terms of the measured  $^1S_0$  scattering length  $a = -23.7$  fm. Note that this expression is very different than the pure OPE calculation.

The renormalization prescription (A.15) is different than  $\overline{MS}$ , but it is straightforward to relate the two. Using

$$\frac{1}{\tilde{C}} - \tilde{G}_E(\mathbf{0}, \mathbf{0}) = \frac{1}{\tilde{C}_{\overline{MS}}} - \tilde{G}_E^{\overline{MS}}(\mathbf{0}, \mathbf{0}) , \quad (\text{A.17})$$

one finds

$$\begin{aligned} \frac{1}{\tilde{C}_{\overline{MS}}} &= \frac{1}{\tilde{C}} - [\tilde{G}_E(\mathbf{0}, \mathbf{0}) - \tilde{G}_E^{\overline{MS}}(\mathbf{0}, \mathbf{0})] \\ &= \frac{1}{\tilde{C}_R(\lambda)} - \mathcal{K}_0^\lambda(0) - [\tilde{G}_0(\mathbf{0}, \mathbf{0}) - G_0^{\overline{MS}}(\mathbf{0}, \mathbf{0})] . \end{aligned} \quad (\text{A.18})$$

Here we used the fact that the difference  $[\tilde{G}_E(\mathbf{0}, \mathbf{0}) - \tilde{G}_E^{\overline{MS}}(\mathbf{0}, \mathbf{0})]$  is independent of  $E$ . Rearranging eq. (A.18) using the fact that only the first two diagrams in the perturbative expansion of  $\tilde{G}_0(\mathbf{0}, \mathbf{0})$  are divergent yields

$$\begin{aligned} \frac{1}{\tilde{C}_{\overline{MS}}} &= \frac{1}{\tilde{C}_R(\lambda)} - \lim_{r' \rightarrow 0} \left[ \mathcal{K}_0^\lambda(r') + \langle \mathbf{r}' | \hat{G}_0^0 | \mathbf{r} = \mathbf{0} \rangle + \langle \mathbf{r}' | \hat{G}_0^0 \hat{V}_\pi \hat{G}_0^0 | \mathbf{r} = \mathbf{0} \rangle \right] \\ &+ \left[ \langle \mathbf{r}' = \mathbf{0} | \hat{G}_0^0 | \mathbf{r} = \mathbf{0} \rangle_{\overline{MS}} + \langle \mathbf{r}' = \mathbf{0} | \hat{G}_0^0 \hat{V}_\pi \hat{G}_0^0 | \mathbf{r} = \mathbf{0} \rangle_{\overline{MS}} \right] . \end{aligned} \quad (\text{A.19})$$

Explicit calculation gives

$$\begin{aligned} \langle \mathbf{r}' | \hat{G}_0^0 | \mathbf{r} = \mathbf{0} \rangle &= \frac{-M}{4\pi r'} , \\ \langle \mathbf{r}' | \hat{G}_0^0 \hat{V}_\pi \hat{G}_0^0 | \mathbf{r} = \mathbf{0} \rangle &= -\frac{\alpha_\pi M^2}{4\pi} [1 - \ln(m_\pi r') - \gamma + \dots] , \end{aligned} \quad (\text{A.20})$$

where the ellipses represent terms that vanish as  $r' \rightarrow 0$ . In eq. (A.20)  $\gamma$  is Euler's constant ( $\gamma \simeq 0.577$ ). Using dimensional regularization

$$\langle \mathbf{r}' = \mathbf{0} | \hat{G}_0^0 | \mathbf{r} = \mathbf{0} \rangle_{\overline{MS}} = 0 \quad (\text{A.21})$$

and

$$\langle \mathbf{r}' = \mathbf{0} | \hat{G}_0^0 \hat{V}_\pi \hat{G}_0^0 | \mathbf{r} = \mathbf{0} \rangle_{\overline{MS}} = -4\pi\alpha_\pi M^2 I_n(m_\pi) , \quad (\text{A.22})$$

where  $I_n(m_\pi)$  is the two loop integral

$$I_n(m_\pi) = \int \frac{d^n \mathbf{q}}{(2\pi)^n} \int \frac{d^n \mathbf{k}}{(2\pi)^n} \frac{1}{\mathbf{q}^2} \frac{1}{\mathbf{k}^2} \frac{1}{[(\mathbf{q} - \mathbf{k})^2 + m_\pi^2]} . \quad (\text{A.23})$$

Combining denominators with the Feynman trick

$$\begin{aligned} I_n(m_\pi) &= \int_0^1 dx \int \frac{d^n \mathbf{q}}{(2\pi)^n \mathbf{q}^2} \int \frac{d^n \mathbf{k}}{(2\pi)^n} \frac{1}{[\mathbf{k}^2 + \mathbf{q}^2 x(1-x) + m_\pi^2 x]^2} \\ &= \int_0^1 dx \int \frac{d^n \mathbf{q}}{(2\pi)^n \mathbf{q}^2} \frac{\pi^{n/2}}{(2\pi)^n} \frac{\Gamma(2-n/2)}{[\mathbf{q}^2 x(1-x) + m_\pi^2 x]^{2-n/2}} . \end{aligned} \quad (\text{A.24})$$

Changing the momentum integration variable from  $\mathbf{q}$  to  $\mathbf{p} = \sqrt{1-x}\mathbf{q}$  the above becomes

$$I_n(m_\pi) = \frac{\pi^{n/2} \Gamma(2-n/2)}{(2\pi)^{2n}} \int_0^1 dx x^{n/2-2} (1-x)^{1-n/2} \int \frac{d^n \mathbf{p}}{\mathbf{p}^2} \frac{1}{[\mathbf{p}^2 + m_\pi^2]^{2-n/2}} . \quad (\text{A.25})$$

Performing the  $\mathbf{p}$  integration and the  $x$  integration gives

$$I_n(m_\pi) = -\frac{\pi^n \Gamma(3-n)(m_\pi^2)^{n-3}}{(2\pi)^{2n}} \Gamma\left(\frac{n}{2} - 1\right) \Gamma\left(1 - \frac{n}{2}\right) . \quad (\text{A.26})$$

Consequently in the  $\overline{MS}$  subtraction scheme

$$\begin{aligned} \langle \mathbf{r}' = \mathbf{0} | \hat{G}_0^0 | \mathbf{r} = \mathbf{0} \rangle_{\overline{MS}} &= 0, \\ \langle \mathbf{r}' = \mathbf{0} | \hat{G}_0^0 \hat{V}_\pi \hat{G}_0^0 | \mathbf{r} = \mathbf{0} \rangle_{\overline{MS}} &= -\frac{\alpha_\pi M^2}{8\pi} \left[ 1 - \ln\left(\frac{m_\pi^2}{\mu^2}\right) \right]. \end{aligned} \quad (\text{A.27})$$

Combining these results and using the small  $r$  behavior of  $\mathcal{K}_0^\lambda(r)$  in eq. (A.3) yields

$$\frac{1}{\tilde{C}_{\overline{MS}}} = \frac{1}{\tilde{C}_R(\lambda)} - \frac{\alpha_\pi M^2}{8\pi} \left[ \ln\left(\frac{\mu^2}{\lambda^2}\right) + 2\gamma - 1 \right] , \quad (\text{A.28})$$

and consequently,

$$G_E^{\overline{MS}}(\mathbf{0}, \mathbf{0}) = \frac{z^*}{y^*} - \frac{\alpha_\pi M^2}{8\pi} \left[ \ln\left(\frac{\mu^2}{\lambda^2}\right) + 2\gamma - 1 \right] . \quad (\text{A.29})$$

The  $\lambda$  dependence of  $1/\tilde{C}_R(\lambda)$  is exactly cancelled by the  $\lambda$  dependence of  $\ln\left(\frac{\mu^2}{\lambda^2}\right)$  appearing in the second term on the r.h.s of (A.28), leaving  $1/\tilde{C}_{\overline{MS}}$  independent of  $\lambda$ . Similarly, cancellation of the  $\lambda$  dependent terms on the r.h.s. of (A.29) leaves  $G_E^{\overline{MS}}(\mathbf{0}, \mathbf{0})$  independent of  $\lambda$ .  $G_E^{\overline{MS}}(\mathbf{0}, \mathbf{0})$  is plotted in fig. 10 for a subtraction point of  $\mu = m_\pi$ .

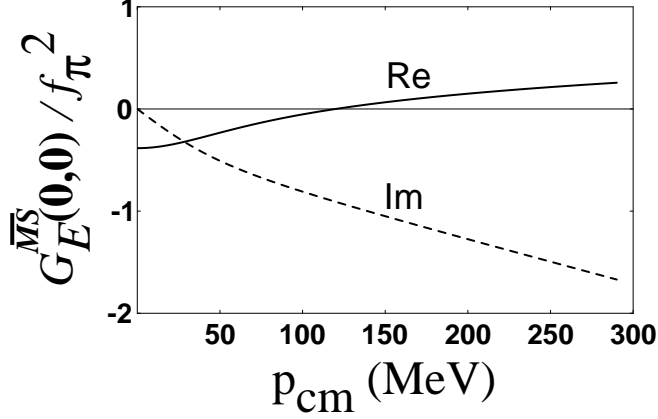


Fig. 10. The  $\overline{MS}$  Green function at the origin normalized to  $f_\pi^2$ ,  $G_E^{\overline{MS}}(\mathbf{0}, \mathbf{0})/f_\pi^2$ , as a function of  $|\mathbf{p}|$  in MeV. The solid and dashed lines are the real and imaginary parts, respectively.

## Appendix B. Computing the effects of 2-derivative, 4-nucleon interactions

In this appendix we show how to compute the sum of ladder diagrams in  $\overline{MS}$  when a two-derivative, 4-nucleon operator is included. Consider the ladder sum including both the contact interactions (3.12) as well as the Yukawa part of one pion exchange:

$$\hat{V} = \hat{V}_\pi + \hat{V}_c, \quad (\text{B.1})$$

where  $\hat{V}_\pi$  is given in eq. (4.4) as

$$\langle \mathbf{p} | \hat{V}_\pi | \mathbf{p}' \rangle = -\frac{4\pi\alpha_\pi}{(\mathbf{p} - \mathbf{p}')^2 + m_\pi^2}, \quad \alpha_\pi = \frac{g_A^2 m_\pi^2}{8\pi f_\pi^2}, \quad (\text{B.2})$$

and  $f_\pi = 132$  MeV is the pion decay constant. (For the effective theory without pions, one can take the result we will derive and set  $\alpha_\pi = 0$ ). The contact interaction  $\hat{V}_c$  is given by,

$$\langle \mathbf{p} | \hat{V}_c | \mathbf{p}' \rangle = \tilde{C} \left( 1 + \frac{\mathbf{p}^2 + \mathbf{p}'^2}{2\Lambda^2} \right). \quad (\text{B.3})$$

This can be conveniently rewritten as

$$V_c(\mathbf{p}, \mathbf{p}') = \tilde{C} (1 + ME/\Lambda^2) - \tilde{C} M \left( \frac{(E - \mathbf{p}^2/M) + (E - \mathbf{p}'^2/M)}{2\Lambda^2} \right), \quad (\text{B.4})$$

or in operator form as

$$\hat{V}_c = \tilde{C} \iint \frac{d^3\mathbf{q}}{(2\pi)^3} \frac{d^3\mathbf{q}'}{(2\pi)^3} \left( (1 + ME/\Lambda^2) |\mathbf{q}\rangle \langle \mathbf{q}'| - \left\{ M(\hat{G}_E^0)^{-1}/\Lambda^2, |\mathbf{q}\rangle \langle \mathbf{q}'| \right\} \right) \quad (\text{B.5})$$

where  $(\hat{G}_E^0)^{-1} = (E - \hat{H}_0)$ .

The first term in eq. (B.4) is easy to deal with, since  $E$  is a number, not an operator. Computing the effects of the second term involving the operator  $(\hat{G}_E^0)^{-1}$  requires some thought. There are three ways the  $(\hat{G}_E^0)^{-1}$  term can enter the ladder diagram calculation.

Firstly, there could be an insertion acting on the “external” legs (by external legs we mean nucleon propagators which interact via  $\hat{V}_\pi$ , but not through any contact interactions). This entails calculating the integral ( $\langle \mathbf{p} |$  is an on-shell state)

$$\begin{aligned} \int \frac{d^n \mathbf{q}}{(2\pi)^n} \langle \mathbf{p} | (\hat{G}_E^0)^{-1} \hat{G}_E (\hat{G}_E^0)^{-1} | \mathbf{q} \rangle &= \int \frac{d^n \mathbf{q}}{(2\pi)^n} \langle \mathbf{p} | (\hat{G}_E^0)^{-1} (1 + \hat{G}_E \hat{V}_\pi) | \mathbf{q} \rangle \\ &= \alpha_\pi m_\pi \int \frac{d^n \mathbf{q}}{(2\pi)^n} \langle \mathbf{p} | (\hat{G}_E^0)^{-1} \hat{G}_E | \mathbf{q} \rangle , \end{aligned} \quad (\text{B.6})$$

where we made use of the fact that  $\langle \mathbf{p} | (\hat{G}_E^0)^{-1} | \mathbf{q} \rangle = 0$  for an on-shell state  $\langle \mathbf{p} |$ ; as well as the dimensionally regulated integral

$$\int \frac{d^n \mathbf{q}}{(2\pi)^n} \langle \mathbf{q}' | \hat{V}_\pi | \mathbf{q} \rangle = \int \frac{d^n \mathbf{q}}{(2\pi)^n} \frac{-4\pi\alpha_\pi}{(\mathbf{q} - \mathbf{q}')^2 + m_\pi^2} = \alpha_\pi m_\pi . \quad (\text{B.7})$$

This is equivalent making the replacement  $(\hat{G}_E^0)^{-1} \rightarrow \alpha_\pi m_\pi$ . (Only the second factor of  $(\hat{G}_E^0)^{-1}$  in eq. (B.6) comes from the interaction  $\hat{V}_\pi$ ; the first  $(\hat{G}_E^0)^{-1}$  is there to amputate the outgoing propagator).

Secondly, one insertion of  $(\hat{G}_E^0)^{-1}$  could act on internal nucleon lines (dressed by  $\hat{V}_\pi$ ). This gives rise to the integral

$$\begin{aligned} \iint \frac{d^n \mathbf{q}}{(2\pi)^n} \frac{d^n \mathbf{q}'}{(2\pi)^n} \langle \mathbf{q} | \hat{G}_E (\hat{G}_E^0)^{-1} | \mathbf{q}' \rangle &= \iint \frac{d^n \mathbf{q}}{(2\pi)^n} \frac{d^n \mathbf{q}'}{(2\pi)^n} \langle \mathbf{q} | (1 + \hat{G}_E \hat{V}_\pi) | \mathbf{q}' \rangle \\ &= \alpha_\pi m_\pi \iint \frac{d^n \mathbf{q}}{(2\pi)^n} \frac{d^n \mathbf{q}'}{(2\pi)^n} \langle \mathbf{q} | \hat{G}_E | \mathbf{q}' \rangle , \end{aligned} \quad (\text{B.8})$$

where we made use of the relation (2.8) between the full and free propagators, of the integral (B.7), and of the fact that  $\int \frac{d^n \mathbf{q}}{(2\pi)^n} \mathbf{q}^{2r} = 0$  in dimensional regularization. Again,  $(\hat{G}_E^0)^{-1}$  just gets replaced by  $\alpha_\pi m_\pi$ .

Finally, two insertions of  $(\hat{G}_E^0)^{-1}$  could act on internal lines:

$$\begin{aligned}
& \iint \frac{d^n \mathbf{q}}{(2\pi)^n} \frac{d^n \mathbf{q}'}{(2\pi)^n} \langle \mathbf{q} | (\hat{G}_E^0)^{-1} \hat{G}_E (\hat{G}_E^0)^{-1} | \mathbf{q}' \rangle \\
&= \iint \frac{d^n \mathbf{q}}{(2\pi)^n} \frac{d^n \mathbf{q}'}{(2\pi)^n} \langle \mathbf{q} | (\hat{G}_E^0)^{-1} (1 + \hat{G}_E \hat{V}_\pi) | \mathbf{q}' \rangle \\
&= \alpha_\pi m_\pi \iint \frac{d^n \mathbf{q}}{(2\pi)^n} \frac{d^n \mathbf{q}'}{(2\pi)^n} \langle \mathbf{q} | (\hat{G}_E^0)^{-1} \hat{G}_E | \mathbf{q}' \rangle \\
&= (\alpha_\pi m_\pi)^2 \iint \frac{d^n \mathbf{q}}{(2\pi)^n} \frac{d^n \mathbf{q}'}{(2\pi)^n} \langle \mathbf{q} | \hat{G}_E | \mathbf{q}' \rangle .
\end{aligned} \tag{B.9}$$

Again we see that  $(\hat{G}_E^0)^{-1}$  gets replaced by  $\alpha_\pi m_\pi$ . In conclusion, given eqs. (B.4), (B.5), the effect of including the 2-derivative operator in eq. (3.1) is simply to replace  $\tilde{C}$  by

$$\tilde{C} \rightarrow \tilde{C} \left( 1 - \frac{\alpha_\pi m_\pi M}{\Lambda^2} + \frac{EM}{\Lambda^2} \right) . \tag{B.10}$$

This is the result utilized in §4. The expression (3.13) in §3 involves the substitution (B.10) with  $\alpha_\pi$  set to zero (no pion contribution).

## References

- [1] S. Weinberg, *Physica* (Amsterdam) 96A (1979) 327; E. Witten, *Nucl. Phys.* B122 (1977) 109.
- [2] H. Georgi, *Ann. Rev. of Nucl. and Part. Sci.*, 43 (1993) 209; J. Polchinski, *Proceedings of Recent Directions in Particle Theory*, TASI92 (1992) 235; A. V. Manohar, *Effective Field Theories*, hep-ph/9508245; D.B. Kaplan, *Effective Field Theories*, hep-ph/9506035.
- [3] S. Weinberg, *Phys. Lett.* 251B (1990) 288; *Nucl. Phys.* B363 (1991) 3; *Phys. Lett.* 295B (1992) 114.
- [4] C. Ordonez, U. van Kolck, *Phys. Lett.* 291B (1992) 459; C. Ordonez, L. Ray, U. van Kolck, *Phys. Rev. Lett.* 72 (1994) 1982; *Phys. Rev. C* 53 (1996) 2086, nucl-th/9511380.
- [5] U. van Kolck, *Phys. Rev.* C49 (1994) 2932.
- [6] W. N. Cottingham *et al*, *Phys. Rev.* D8 (1973) 800.
- [7] R. Machleidt, K. Holinde and C. Elster, *Phys. Rep.* 149 (1987) 1.
- [8] M.M. Nagels, T.A. Rijken and J.J. de Swart, *Phys. Rev.* D17 (1978) 768.
- [9] U. van Kolck, J.L. Friar and T. Goldman, *Phys. Lett.* 371B (1996) 169.
- [10] M.J. Savage and M.B. Wise, *Phys. Rev.* D53 (1996) 349.
- [11] T.-S. Park, D.-P. Min and M. Rho, *Phys. Rept.* 233 (1993) 341; T.-S. Park, I. S. Towner and K. Kubodera, *Nucl. Phys.* A579 (1994) 381; T.-S. Park, D.-P. Min and M. Rho, *Phys.Rev.Lett.*74 (1995) 4153; T.-S. Park, D.-P. Min and M. Rho, *Nucl.Phys.*A596 (1996) 515.
- [12] J.L. Friar, D.G. Madland and B.W Lynn, nucl-th/9512011 (1995).
- [13] J.L. Friar, *Nuclear Forces and Chiral Theories*, Few-Body Systems Suppl. 99 (1996) 1.
- [14] U. van Kolck, *Effective Chiral Theory of Nuclear Forces*, Lectures presented at the 7th Summer School and Symposium on Nuclear Physics, Seoul, (1994).
- [15] M.L. Goldberger and K.M Watson, *Collision Theory*, John Wiley and Sons, Inc. (1964).
- [16] M.A. Preston and R.K. Bhaduri, *Structure of the Nucleus*, Addison-Wesley Publishing Company, Reading, Massachusetts (1975); 2nd printing (1982).
- [17] Partial wave analysis of the Nijmegen University theoretical high energy physics group, obtained from WorldWide Web page <http://nn-online.sci.kun.nl/>
- [18] J.L. Gervais and B. Sakita, *Phys. Rev. Lett.* 52 (1984) 87; R. Dashen and A.V. Manohar, *Phys. Lett.* 315B (1993) 425.
- [19] D.B. Kaplan and M.J. Savage, *Phys. Lett.* 365B (1995) 244.
- [20] G. Baym and D.K. Campbell, in *Mesons and Nuclei*, edited by M. Rho and D. Wilkinson, North Holland Pub. Co. (1979) 1031.
- [21] D.B. Kaplan and A.E. Nelson, *Phys. Lett.* 175B (1986) 57.

- [22] H. D. Politzer and M.B. Wise, Phys. Lett. 273B (1991) 156; D. Montano, H.D. Politzer and M.B. Wise, Nucl. Phys. B375 (1992) 507.
- [23] G.E. Brown, C.-H. Lee, M. Rho and V. Thorsson, Nucl. Phys. A567 (1994) 937; C.-H. Lee, G.E. Brown, D.-P. Min and M. Rho, Nucl. Phys. A585 (1995) 401.
- [24] T. E. O. Ericson and L. Hambro, Ann. Phys. 107 (1977) 44.